Geochimica et Cosmochimica Acta, Vol. 69, No. 19, pp. 4685–4701, 2005

0016-7037/05 $30.00 + .00

doi:10.1016/j.gca.2005.02.006

Platinum-group element constraints on source composition and magma evolution of the Kerguelen Plateau using basalts from ODP Leg 183

William J. Chazey III and Clive R. Neal*
Department of Civil Engineering and Geological Sciences, University of Notre Dame, Notre Dame, IN 46556, USA

(*Received February* 23, 2004; *accepted in revised form February* 14, 2005)

Abstract—Seventeen basalts from Ocean Drilling Program (ODP) Leg 183 to the Kerguelen Plateau (KP) were analyzed for the platinum-group elements (PGEs: Ir, Ru, Rh, Pt, and Pd), and 15 were analyzed for trace elements. Relative concentrations of the PGEs ranged from ~0.1 (Ir, Ru) to ~5 (Pt) times primitive mantle. These relatively high PGE abundances and fractionated patterns are not accounted for by the presence of sulfide minerals; there are only trace sulfides present in thin-section. Sulfur saturation models applied to the KP basalts suggest that the parental magmas may have never reached sulfide saturation, despite large degrees of partial melting (~30%) and fractional crystallization (~45%).

First order approximations of the fractionation required to produce the KP basalts from an ~30% partial melt of a spinel peridotite were determined using the PELE program. The model was adapted to better fit the physical and chemical observations from the KP basalts, and requires an initial crystal fractionation stage of at least 30% olivine plus Cr-spinel (49:1), followed by magma replenishment and fractional crystallization (RFC) that included clinopyroxene, plagioclase, and titanomagnetite (15:9:1). The low Pd values ($[Pd/Pt]_{pm} < 1.7$) for these samples are not predicted by currently available K_d values. These Pd values are lowest in samples with relatively higher degrees of alteration as indicated by petrographic observations. Positive anomalies are a function of the behavior of the PGEs; they can be reproduced by Cr-spinel, and titanomagnetite crystallization, followed by titanomagnetite resorption during the final stages of crystallization. Our modeling shows that it is difficult to reproduce the PGE abundances by either depleted upper or even primitive mantle sources. Crustal contamination, while indicated at certain sites by the isotopic compositions of the basalts, appears to have had a minimal affect on the PGEs. The PGE abundances measured in the Kerguelen Plateau basalts are best modeled by melting a primitive mantle source to which was added up to 1% of outer core material, followed by fractional crystallization of the melt produced. This reproduces both the abundances and patterns of the PGEs in the Kerguelen Plateau basalts. An alternative model for outer core PGE abundances requires only 0.3% of outer core material to be mixed into the primitive mantle source. While our results are clearly model dependent, they indicate that an outer core component may be present in the Kerguelen plume source.

1. INTRODUCTION

Large igneous provinces (LIPs; Coffin and Eldholm, 1993, 1994) are usually associated with hotspots and are generally considered to be the product of initial plume magmatism (cf. Richards et al., 1989). Plumes are generated through heat transfer across a boundary layer, which causes thermal instability resulting in diapiric rise of a large buoyant mass of hot mantle material (cf. Campbell and Griffiths, 1990). The plume is composed of a "head" and a smaller "tail." Melting of the plume head as it approaches or impacts the lithosphere initiates surface magmatism by thinning the overlying mantle and crust through lateral spreading and/or thermal erosion (Saunders et al., 1994). This magmatism may occur almost continuously for millions of years (e.g., Kerguelen Plateau [KP]; Frey and Weis, 1995; Weis et al., 1998; Frey et al., 2000a; Duncan 2002) or occur in discrete events (e.g., Ontong Java Plateau [OJP], Mahoney et al., 1993; Tejada et al., 1996, 2002; Birkhold, 2000). Not all LIPs have a surface expression of the plume tail (i.e., a hotspot track). In the case of the largest terrestrial LIPs, it has been suggested that the tremendous volume of material erupted (OJP: c. 5×10^7 km^3, M. Coffin, personal communication, 2003) requires a source in the lower mantle or even at the core-mantle boundary (Coffin and Eldholm, 1993, 1994). Indeed, outer core material has been proposed as a contaminant in the source of some plumes (e.g., Walker et al., 1995; Brandon et al., 1999; Ely and Neal, 2003; Chazey and Neal, 2004).

Due to the immense size of the rising diapirs that produce these provinces, and the extent and duration of the resultant volcanism, most LIPs have incorporated material compositionally distinct from the plume itself. However, the amount of incorporated/assimilated material (if any) is the subject of some debate (Farnetani et al., 2002; Kumagai, 2002). The plume head entrains portions of the mantle through which it passes (Campbell and Griffiths, 1990), giving rise to heterogeneities in the source before melting is initiated. The composition of the entrained material can vary significantly, depending upon the depth of its origin. Once the plume intersects with the base of the lithosphere and begins to melt, it may interact with a midocean ridge, taking advantage of this preexisting path to the surface (e.g., Iceland). Assimilation of lithospheric material is often promoted by the excess heat associated with plumes. For example, in the case of the Kerguelen plume it experienced lithospheric mantle/crustal contamination, with the contami-

* Author to whom correspondence should be addressed, at University of Notre Dame, Department of Civil Engineering and Geological Sciences, 156 Fitzpatrick Hall, Notre Dame, IN 45556, USA (neal.1@nd.edu).

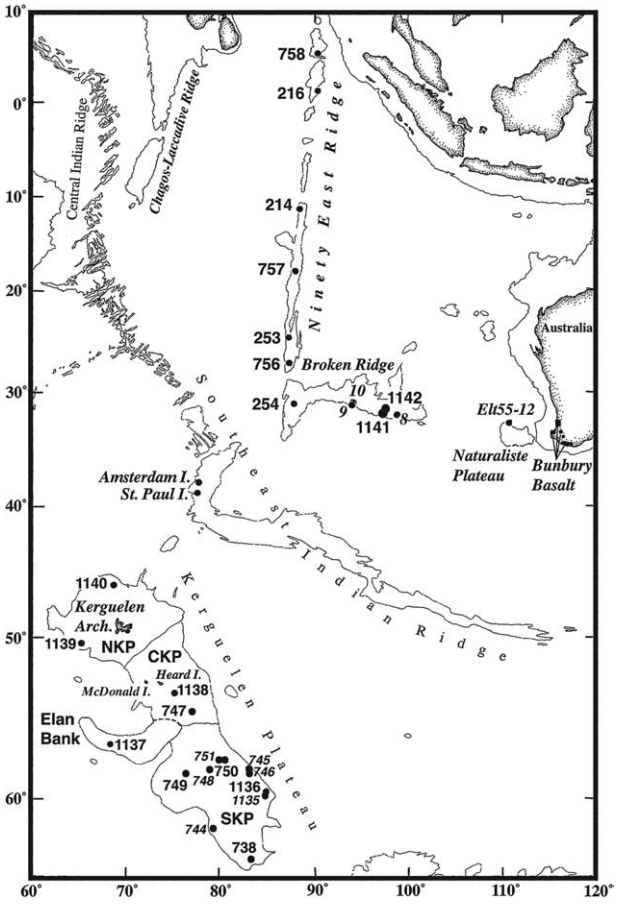

Fig. 1. Map of the Kerguelen Plateau, Broken Ridge, and other features associated with the Kerguelen plume. Numbered points represent Deep Sea Drilling Project (DSDP) and Ocean Drilling Program (ODP) drill and dredge sites (adapted from Neal et al., 2002). Samples for this study are taken from Sites 1136, 1137, 1138, 1141 and 1142.

nants having been defined using a combination of trace element and isotopic signatures (Frey et al., 2002; Neal et al., 2002; Weis and Frey, 2002).

In this paper, we use the platinum-group elements (PGEs; Ir, Ru, Rh, Pt, and Pd) to explore the possibility that a small outer core component may be present in the Kerguelen Plateau through the analysis of 17 samples returned from Ocean Drilling Program (ODP) Leg 183. The samples analyzed are from Sites 1136, 1137, and 1138 on the KP, and Sites 1141 and 1142 on Broken Ridge (Fig. 1). The use of PGE abundances and patterns to assess core involvement in a mantle plume has previously been applied to the OJP (Ely and Neal, 2003; Chazey and Neal, 2004). In the case of the Kerguelen Plateau, we will show that the basalts are relatively enriched in the PGEs, which exhibit lithophile behavior during magmatic evolution. Illustrative modeling of PGE abundances and normalized profiles is conducted to explore the feasibility of an outer core component being present in these basalts.

2. BACKGROUND

The Kerguelen Plateau is a northwest-southeast trending basaltic province, ~2300 km long by 200–600 km wide, covering ~1.5 × 10^6 km^2 in the southern Indian Ocean (Fig. 1). Ocean Drilling Program (ODP) Leg 183 drilled eight sites (1135–1142; Fig. 1), seven of which recovered basement (Coffin et al., 2000). Aside from recent volcanism (e.g., the Kerguelen Archipelago, 30–0 Ma), the bulk of the KP is currently submarine, although ODP Leg 183 found evidence that currently submarine portions of the KP were once above sea level during their formation (Frey et al., 2000a; Mohr et al., 2002). The initial phase of KP magmatism began at ~118–119 Ma during the breakup of Antarctica, Australia, and India, creating what is now the southern portion of the plateau (Duncan, 2002) and the Rajmahal Traps in Northern India (Kent et al., 2002). This upper age limit may be extended (to ~130 Ma) if the Bunbury basalts in southeastern Australia owe their origin to the Kerguelen hotspot (Mahoney et al., 1983; Frey et al., 1996). The basalts from Elan Bank in the western KP erupted at ~108 Ma (Duncan, 2002) and contained unequivocal evidence of continental crust involvement (e.g., Nicolaysen et al., 2001; Weis et al., 2001; Ingle et al., 2002). The central section of the KP was formed at 101–102 Ma (Site 1138), followed by Broken Ridge at 94–95 Ma, which was split from the central KP during the opening of the Southeast Indian Ridge (SEIR) at ~42 Ma and now lies well to the northeast of the KP (Pringle and Duncan, 2000; Duncan, 2002). At 82 Ma, another feature associated with the Kerguelen plume, the Ninetyeast Ridge, also began to form (Weis et al., 1991). The SEIR was moving northward at the time, but maintained its position relative to the plume with several southward ridge jumps (Royer et al., 1991). A ridge jump at ~38 Ma terminated the formation of the Ninetyeast ridge (Mahoney et al., 1995). The northern part of the KP formed at ~40 Ma (Duncan, 2002), while the Kerguelen Archipelago has been erupting since 30 Ma with the strongest period of magmatism between 29 and 25 Ma (Weis et al., 1998; Frey et al., 2000b). Present-day volcanic activity is primarily limited to the islands of Heard and McDonald to the southeast of the archipelago (Barling et al., 1994). The Ninetyeast Ridge, Kerguelen Archipelago, and McDonald and Heard Islands represent the volcanic activity of the tail of the Kerguelen plume. These features, along with the KP, represent ~120 m.y. of continuous plume activity.

Results from the ODP Leg 119, 120, and 183 Kerguelen Plateau basement samples (see Fig. 1 for site locations) together with previous results from dredging (Davies et al., 1989; Weis et al., 1989, 2002) suggest that the KP has had a very complex history. The south and central KP are comprised of tholeiitic to transitional basalts, while the northern KP and the Kerguelen Archipelago become more alkalic with decreasing age (Weis et al., 1993, 1998; Frey et al., 2000b). All of the KP basalts are evolved, with an MgO content ranging from 4 to 9 wt%, with most recent Kerguelen Archipelago basalts containing a higher proportion of more evolved compositions. Modeling of these young, evolved basalts also indicates a lower degree of partial melting produced the lavas that formed the archipelago relative to earlier KP basalts, suggesting a decreasing heat supply from the KP hotspot over time (Frey et al., 2000b).

Three compositionally distinct reservoirs have been involved in the generation of the KP, as inferred from isotope data: the plume itself, the SEIR (which affected the north of the KP) and continental material (which affected the south and west portion

of the KP). The plume component has been defined as having a relatively enriched mantle isotopic signature (Salters et al., 1992; Weis et al., 1993, 2002; Mahoney et al., 1995; Frey and Weis, 1995, 1996; Mattielli et al., 1999), intermediate between EMI and EMII in a Sr-Nd isotopic diagram. Weis et al. (1998) proposed that the uncontaminated Kerguelen plume signature (the plume tail) is best represented by the combined isotopic ranges of the Upper Miocene Series (10.2–6.6 Ma) and Mount Ross rocks (1–0.1 Ma) of the Kerguelen Archipelago. Subsequently, Neal et al. (2002), used isotope data and trace element ratios to suggest that the alkali basalts at Sites 1141 and 1142 on Broken Ridge represent the pure plume signature [($^{87}Sr/^{86}Sr)_t$ = 0.70533–0.70566, $\varepsilon_{Nd}(t)$ = +0.3 to +0.5, ($^{206}Pb/^{204}Pb)_t$ = 17.989–18.022, ($^{207}Pb/^{204}Pb)_t$ = 15.586–15.611, ($^{208}Pb/^{204}Pb)_t$ = 38.593–38.770, $(La/Nb)_{pm}$ and $(Th/Ta)_{pm} < 1$, where pm denotes primitive mantle-normalized and t represents age-corrected isotope data].

In the south and west of the KP (Sites 738 and 1137; Fig. 1), isotopic data indicate a strong continental influence (Storey et al., 1992; Ingle et al., 2002). Strontium and Nd isotopes show strong enrichments, plotting beyond EMI and EMII towards continental material (Weis et al., 1993; Mahoney et al., 1995). The basalts at these sites have high $^{207}Pb/^{204}Pb$ values for given $^{206}Pb/^{204}Pb$, which is also consistent with continental crust (Ingle et al., 2002). Unradiogenic Os isotope signatures from Mont Trapeze harzburgite xenoliths suggest that there may be pieces of Gondwanaland subcontinental lithosphere underlying the Kerguelen Archipelago (Hassler and Shimizu, 1998). The only direct evidence of continental crust being present at the formation of the KP is at Elan Bank, where garnet gneiss is present as cobbles in an interflow conglomerate (Coffin et al., 2000; Nicolaysen et al., 2001; Weis et al., 2001).

Trace element data for the Kerguelen Plateau basalts are consistent with the isotopic data. Ratios such as $(La/Nb)_{pm}$ and $(Th/Ta)_{pm}$ should be ~1 for mantle-derived basalts (e.g., Sun and McDonough, 1989; McDonough and Sun, 1995). However, basalt samples from across the KP, including Broken Ridge, have values for these ratios that decrease from ~2 where there is a continental crust influence (Site 738) to more typical ocean island basalt (OIB) values at ~1 (Salters et al., 1992; Mahoney et al., 1995). As mentioned above, enrichment of Sr, Nd, and $^{207/204}Pb$ for a given $^{206/204}Pb$ towards continental crust values also occurs in these samples, with this influence decreasing to the north and east. Samples from Site 1140 have been interpreted as being derived from a source containing 63%–99% of a depleted mantle component, and have compositions that are considered to be intermediate between the enriched plume signature and the SEIR (Weis and Frey, 2002). Isotopic characteristics also shift to this more MORB-like signature.

3. ANALYTICAL TECHNIQUES

Samples were chosen on the basis of being the least altered available from each unit. Several grams of each of the samples analyzed were prepared as described in Chazey et al. (2003). The amount of powder varied from sample to sample, but to minimize the PGE nugget effect (cf. Tredoux and McDonald, 1996), no less than ~3 g of sample were powdered. Two hundred and fifty milligrams of each sample powder and the CANMET PGE reference material UMT-1 were then dissolved in sequential stages and analyzed by inductively coupled plasma mass spectrometry (ICP-MS; Fisons PlasmaQuad II+) as described by Ely et al. (1999). The PGE data were reduced using the method of Ely and Neal (2001), which gives realistic error analysis for each sample and standard analyzed. Unless otherwise noted, the isotopes that were analyzed to determine the total element concentrations presented in Table 1 are ^{102}Ru, ^{103}Rh, ^{105}Pd, ^{191}Ir, and ^{195}Pt. For details regarding the analytical procedures used in determining the trace element contents of the samples discussed in this paper, see Jenner et al. (1990) and Neal (2001). Trace element concentrations for the Site 1137 garnet gneiss were determined using ICP-MS analysis of $LiBO_2$ fusions as described in Neal et al. (2002). Major element data were acquired via X-ray fluorescence at the University of Massachusetts at Amherst following the methods described by Rhodes (1996).

4. PETROGRAPHY

The Kerguelen samples analyzed (Table 1) are generally seriate or sparsely to moderately plagioclase- and clinopyroxene-phyric basalts. In-depth petrographic summaries can be found in Coffin et al. (2000) and Neal et al. (2002). We present a brief summary here.

Samples near the edges of a flow or pillow unit generally have intergranular or intersertal textures; less-commonly they are trachytic or subtrachytic. Samples from the interiors of these units tend to have a somewhat larger grain size and subophitic to intergranular or intersertal textures. These coarser grained basalts are dominated by subhedral to anhedral plagioclase in the groundmass, ranging from 45 to 70 modal % of each sample, while partially altered anhedral clinopyroxene (15–40 modal %) and devitrified glass make up the bulk of the remaining portion. Plagioclase and olivine (<5 modal %) phenocrysts are found both as isolated crystals and in some cases as glomerocrysts (e.g., 1136 18R-6 Pc.2, 19–24 cm). Clinopyroxene phenocrysts are partially resorbed in most cases. Total phenocrysts range from none in some samples at Sites 1138 and 1141 to almost 20% in samples from Site 1136. Reflected light microscopy revealed that the all the KP basalts examined contain 1%–4% subhedral, partially resorbed titanomagnetite. Primary sulfides are present as minute (50 μm maximum size and impossible to polish well enough to identify) interstitial blebs, but are rare (<<1 modal %).

4.1. Site 1136

The three basalt units are sparsely to moderately plagioclase-phyric, with lesser amounts of clinopyroxene and olivine (Coffin et al., 2000). Olivine is only found as an altered phenocryst phase in Unit 1. Phenocrysts occur either as individual crystals or glomerocrystic intergrowths. These occur in an intergranular to granular groundmass of clinopyroxene, titanomagnetite, plagioclase, with or without altered glass.

4.2. Site 1137

Two samples from Site 1137 on Elan Bank were analyzed. Sample 1137A 26R1, Pc4, Unit 2B is an aphyric tholeiitic basalt that exhibits an intergranular to intersertal texture of plagioclase, clinopyroxene, titanomagnetite, and variably altered mesostasis. The second sample, 1137A 36R1, 32–37, is a relatively coarse-grained garnet-biotite gneiss cobble from an interflow conglomerate (Coffin et al., 2000). It contains poikiloblastic garnets set in a xenoblastic groundmass of K-feldspar, plagioclase, and quartz, with accessory zircon. The groundmass exhibits a weakly gneissic texture.

Table 1. Platinum-group (ng/g), major (wt%), and trace element (μg/g) abundances for the ODP Leg 183 basalts analyzed in this study.[a]

Leg	Site	Hole	Core	Section	Piece	Interval (cm)	Unit	Type	Ir	2σ	Ru	2σ	Rh	2σ	Pt	2σ	Pd	2σ
183	1136	A	16R	2	2A	24–30	1	tholeiitic	0.75	0.14	1.04	0.12	0.85	0.05	8.2	0.3	7.4	0.4
183	1136	A	18R	6	2	19–24	2	tholeiitic	BDL	BDL	0.35	0.14	0.40	0.04	7.8	1.6	5.6	1.1
183	1137	A	26R	1	4	37–43	2B	tholeiitic?	0.97	0.56	0.97	0.53	1.42	0.27	32.6	6.7	15.4	4.5
183	1137	A	36R	1	1A	32–37	6	garnet-biotite gneiss	BDL	BDL	0.58	0.39	0.31	0.26	18.3	4.8	6.1	1.9
183	1138	A	80R	1	7	39–42	3	tholeiitic	2.08	0.67	1.56	0.37	1.27	0.40	15.3	8.0	9.2	1.0
183	1138	A	80R	5	1	4–11	5	tholeiitic	0.60	0.31	0.28	0.25	0.37	0.26	12.8	4.1	8.4	1.5
183	1138	A	81R	4	12	116–120	7	tholeiitic	1.35	0.30	1.07	0.07	0.83	0.08	17.5	0.8	8.9	1.0
183	1138	A	82R	5	7B	75–84	9	tholeiitic	BDL	BDL	BDL	BDL	0.63	0.31	11.5	3.3	8.2	2.8
183	1138	A	84R	1	5B	67–70	12	tholeiitic	0.88	0.46	0.69	0.36	BDL	BDL	19.1	1.5	11.7	2.4
183	1138	A	85R	1	9	83–87	14	tholeiitic	BDL	BDL	0.48	0.24	BDL	BDL	5.8	2.6	6.5	3.4
183	1138	A	86R	3	6	36–40	17	tholeiitic	0.51	0.14	BDL	BDL	0.38	0.23	10.6	1.5	7.1	3.9
183	1138	A	88R	2	10	134–137	21	tholeiitic	0.42	0.16	0.35	0.12	BDL	BDL	17.9	4.5	8.3	3.8
183	1138	A	89R	3	1A	6–11	22	tholeiitic	0.93	0.65	0.68	0.13	0.42	0.04	19.0	0.9	6.0	1.5
183	1141	A	21R	2	1D	114–125	5	alkalic	BDL	BDL	0.39	0.06	0.25	0.10	6.7	4.6	7.2	1.9
183	1141	A	24R	2	2A	31–34	6	alkalic	0.47	0.13	0.52	0.25	0.36	0.14	12.8	1.4	8.1	1.6
183	1142	A	2R	1	2A	7–11	1	alkalic	0.85	0.14	1.12	0.22	0.54	0.09	18.3	1.7	11.7	1.6
183	1142	A	10R	3	1	12–22	6	tholeiitic	0.50	0.09	0.32	0.20	0.18	0.04	10.6	2.8	3.5	0.8
								UMT-1 (n = 13)	9.1	0.3	10.6	0.4	10.8	0.4	118	4	104	4
								UMT-1 (cert.)	8.8	0.6	10.9	1.5	9.5	1.5	129	5	106	3

Leg	Site	Hole	Core	Section	Piece	Interval (cm)	Unit	Type	MgO	TiO_2	Fe_2O_3	Sc	V	Cr	Co	Ni	Cu	Zn	Rb	Sr
183	1136	A	16R	2	2A	24–30	1	tholeiitic	6.56	1.75	11.96	36.2	278	170	46.0	65.3	49	112	4.10	229
183	1136	A	18R	6	2	19–24	2	tholeiitic	6.65	1.65	12.77	36.2	193	171	48.9	59.8	118	111	4.00	232
183	1137	A	26R	1	4	37–43	2B	tholeiitic?				32.7	295	99	49.2	30.0	45	133	12.8	565
183	1137	A	36R	1	1A	32–37	6	garnet-biotite gneiss				70	50	3.2	5.7	14.5	8.2	46	117	83
183	1138	A	80R	1	7	39–42	3	tholeiitic	5.17	1.92	11.96	48.5	373	86	50.9	57.3	139	130	2.0	234
183	1138	A	80R	5	1	4–11	5	tholeiitic	5.76	2.16	11.58	55.8	509	101	50.7	67.0	157	147	1.3	254
183	1138	A	81R	4	12	116–120	7	tholeiitic	6.37	2.04	13.12	47.5	369	70	47.2	57.6	189	133	11.2	205
183	1138	A	82R	5	7B	75–84	9	tholeiitic	5.83	2.12	14.91	49.1	547	49	56.9	50.9	204	162	6.5	205
183	1138	A	84R	1	5B	67–70	12	tholeiitic	5.98	2.32	13.94	48.3	409	56	48.7	43.8	180	148	5.4	245
183	1138	A	85R	1	9	83–87	14	tholeiitic	5.97	2.56	15.17	40.2	465	46	46.5	35.1	202	162	4.9	210
183	1138	A	86R	3	6	36–40	17	tholeiitic	5.20	2.72	16.92	46.7	578	16	51.2	32.6	209	188	2.8	211
183	1138	A	88R	2	10	134–137	21	tholeiitic	4.96	2.95	17.54	39.7	360	11	52.6	25.6	184	153	2.6	214
183	1138	A	89R	3	1A	6–11	22	tholeiitic	4.74	3.05	17.24	43.6	393	45	51.8	28.2	238	175	3.1	231
183	1141	A	21R	2	1D	114–125	5	alkalic	6.03	2.81	12.38	29.3	218	300	58.9	208	194	126	6.7	523
183	1141	A	24R	2	2A	31–34	6	alkalic	6.45	2.74	11.80	28.6	216	355	47.7	195	173	109	8.7	443
183	1142	A	2R	1	2A	7–11	1	alkalic	7.41	2.78	12.24	30.2	386	405	55.8	220	256	121	14.0	460
183	1142	A	10R	3	1	12–22	6	tholeiitic	4.21	2.57	13.31	33.5	404	21	64.8	40.5	171	142	3.2	204

Table 1. (Continued)

Leg	Site	Hole	Core	Section	Piece	Interval (cm)	Unit	Type	Y	Zr	Nb	Cs	Ba	La	Ce	Pr	Nd	Sm	Eu	Gd
183	1136	A	16R	2	2A	24–30	1	tholeiitic	25.8	93	6.1	0.06	72	7.5	17.2	2.61	12.6	3.64	1.45	4.55
183	1136	A	18R	6	2	19–24	2	tholeiitic	27.1	101	6.2	0.13	81	8.5	20.2	2.96	13.8	4.03	1.44	5.07
183	1137	A	26R	1	4	37–43	2B	tholeiitic?	28.1	203	15.8	0.06	344	23.5	48.2	7.11	29.6	6.58	2.30	7.04
183	1137	A	36R	1	1A	32–37	6	garnet-biotite gneiss	*56*	*209*	*15.5*	2.04	806	66.1	92.0	15.4	52.3	8.91	2.13	7.58
183	1138	A	80R	1	7	39–42	3	tholeiitic	32.8	124	11.2	0.01	81	11.0	25.9	3.83	17.1	4.49	1.58	5.33
183	1138	A	80R	5	1	4–11	5	tholeiitic	30.8	138	12.7		104	11.2	26.8	3.91	17.7	4.61	1.66	5.41
183	1138	A	81R	4	12	116–120	7	tholeiitic	29.3	120	11.5	0.13	117	11.2	27.5	3.85	17.5	4.70	1.71	5.46
183	1138	A	82R	5	7B	75–84	9	tholeiitic	33.7	151	12.9	0.12	86	13.9	29.9	4.49	19.9	5.08	1.76	5.92
183	1138	A	84R	1	5B	67–70	12	tholeiitic	36.2	166	15.6	0.01	99	14.3	36.2	5.28	23.0	5.80	1.99	6.78
183	1138	A	85R	1	9	83–87	14	tholeiitic	48.2	203	17.2	0.11	107	16.9	42.4	6.22	26.4	6.65	2.07	7.99
183	1138	A	86R	3	6	36–40	17	tholeiitic	48.5	265	21.8	0.47	110	19.3	42.4	6.47	28.8	7.30	2.35	8.40
183	1138	A	88R	2	10	134–137	21	tholeiitic	45.5	225	20.6	0.11	115	20.7	51.5	7.40	30.5	7.85	2.32	8.89
183	1138	A	89R	3	1A	6–11	22	tholeiitic	52.2	231	22.7	0.03	125	23.2	55.2	7.67	32.1	8.37	2.60	9.53
183	1141	A	21R	2	1D	114–125	5	alkalic	27.2	132	25.9	0.09	264	20.5	52.7	7.48	31.9	7.01	2.19	7.12
183	1141	A	24R	2	2A	31–34	6	alkalic	27.6	161	25.6	0.22	338	22.3	53.6	7.87	33.6	7.23	2.28	7.28
183	1142	A	2R	1	2A	7–11	1	alkalic	28.5	223	26.8	0.16	260	21.3	55.4	7.78	33.3	7.59	2.35	7.47
183	1142	A	10R	3	1	12–22	6	tholeiitic	26.9	193	15.6	0.08	313	21.5	44.5	6.12	24.1	5.53	2.05	6.61

Leg	Site	Hole	Core	Section	Piece	Interval (cm)	Unit	Type	Th	Dy	Ho	Er	Tm	Yb	Lu	Hf	Ta	Pb	Th	U
183	1136	A	16R	2	2A	24–30	1	tholeiitic	0.80	4.91	0.98	2.75	0.41	2.55	0.31	2.57	0.35	1.42	0.93	0.08
183	1136	A	18R	6	2	19–24	2	tholeiitic	0.88	5.21	1.02	3.00	0.43	2.67	0.40	2.65	0.51	2.39	1.02	0.22
183	1137	A	26R	1	4	37–43	2B	tholeiitic?	0.98	5.90	1.07	2.90	0.34	2.28	0.31	5.61	0.96	3.99	2.66	0.46
183	1137	A	36R	1	1A	32–37	6	garnet-biotite gneiss	0.89	4.80	0.75	1.76	0.17	1.46	0.17	6.35	1.51	18.1	31.8	2.09
183	1138	A	80R	1	7	39–42	3	tholeiitic	0.92	5.73	1.26	3.64	0.54	3.19	0.49	3.36	0.66	0.48	1.02	0.18
183	1138	A	80R	5	1	4–11	5	tholeiitic	0.89	5.62	1.15	3.32	0.50	3.41	0.44	3.46	0.70	1.21	1.00	0.14
183	1138	A	81R	4	12	116–120	7	tholeiitic	0.96	5.90	1.25	3.46	0.53	3.53	0.48	3.38	0.72	1.34	1.24	0.24
183	1138	A	82R	5	7B	75–84	9	tholeiitic	1.00	6.25	1.34	3.82	0.52	3.94	0.51	3.85	0.70	1.62	1.32	0.25
183	1138	A	84R	1	5B	67–70	12	tholeiitic	1.15	7.30	1.56	4.29	0.59	4.97	4.52	0.88	1.98	1.69	0.31	
183	1138	A	85R	1	9	83–87	14	tholeiitic	1.31	8.46	1.78	5.09	0.72	4.94	0.69	5.41	1.04	3.75	1.95	0.48
183	1138	A	86R	3	6	36–40	17	tholeiitic	1.40	8.55	1.83	5.07	0.76	5.29	0.71	5.89	1.10	2.93	2.44	0.50
183	1138	A	88R	2	10	134–137	21	tholeiitic	1.51	9.35	1.98	5.72	0.78	5.62	0.78	6.41	1.32	3.94	2.37	0.50
183	1138	A	89R	3	1A	6–11	22	tholeiitic	1.53	9.80	2.11	5.96	0.83	5.69	0.83	6.00	1.21	3.20	2.39	0.54
183	1141	A	21R	2	1D	114–125	5	alkalic	1.00	5.71	1.06	2.77	0.35	2.52	0.35	3.56	1.53	2.27	1.06	0.15
183	1141	A	24R	2	2A	31–34	6	alkalic	1.01	6.26	1.16	3.23	0.40	2.53	0.39	4.02	1.64	2.40	1.20	0.22
183	1142	A	2R	1	2A	7–11	1	alkalic	1.02	5.86	1.10	3.02	0.43	2.58	0.36	5.87	1.60	3.52	1.15	0.32
183	1142	A	10R	3	1	12–22	6	tholeiitic	1.04	6.31	1.27	3.85	0.59	3.95	0.57	4.93	0.98	4.50	3.64	0.56

[a] Concentrations between the limit of detection (LOD: blank + 3σ) and limit of quantification (LOQ: blank plus 10σ) are reported in italics: those below detection limits are listed as BDL. All PGE abundances are also reported with a 2 sigma value. An average (n = 13) of the standard UMT-1 is reported with certified values for comparison. Underlined values are informational only.

4.3. Site 1138

As noted by Neal et al. (2002), Site 1138 basalts are generaaly aphyric to sparsely plagioclase-clinopyroxene-titanomagnetite phyric. Plagioclase is present either as solitary crystals or as glomerocrysts. Olivine microphenocrysts, partially to completely replaced by clay minerals, are present in Units 5–16 and Unit 19. The phenocrysts exhibit resorption features.

4.4. Sites 1141 and 1142

At Site 1141, Units 2–4 are aphyric to plagioclase-phyric basalts. The base of Unit 4 and Units 5 and 6 contained partially altered olivine as a persistent phenocryst phase (Coffin et al., 2000). The phenocrysts are set in an intersertal to intergranular groundmass of clinopyroxene, plagioclase, titanomagnetite and variably altered glass. A minor, yet common accessory phase is apatite, which is present as minute needles, consistent with the alkalic nature of these basalts. Site 1142 basalts are more altered than those from Site 1141, although relatively unaltered selvages were present in the drill core. The samples analyzed in this study were from Units 1 and 6. Unit 1 is sparsely olivine phyric, with rare plagioclase phenocrysts, and exhibits an intergranular texture. Olivine phenocrysts exhibit only minor alteration to clay minerals. Unit 6 is an aphyric to sparsely plagioclase-phyric tholeiitic pillow basalt.

Samples from Sites 1141 and 1142 contain olivine crystals (<1 modal %), many of which enclose unaltered Cr-spinel crystals (<<1% modal abundance). Cr-spinel was noted in all samples from Sites 1141 and 1142, except sample 1142 10R3 Pc. 1 (Unit 6), which is consistent with the Cr contents of the basalts analyzed from these sites (300–405 μg/g and 21 μg/g, respectively; Neal et al., 2002). These crystals are remnants of an earlier stage of crystallization (olivine + Cr-spinel) experienced by all of the KP basalts, even though Cr-spinel is not represented in all the basalts.

5. RESULTS

The KP basalts analyzed from Sites 1136, 1137, 1138, 1141, and 1142 range from tholeiitic to alkalic and have relatively low MgO (~4.2–7.4 wt%, Table 1), Ni (25.6–220 μg/g) and Co (46.0–64.8 μg/g) abundances, suggesting that the basalts have experienced olivine removal. Samples from Broken Ridge (Sites 1141 and 1142) generally have higher Cr and Ni abundances (300–405 and 195–220 μg/g, respectively) than most of the other basalts analyzed (11–101 and 25.6–67.0 μg/g). The only exception are the Site 1136 basalts, which have intermediate Cr content (170–171 μg/g). The Site 1136 basalts also contain the lowest REE, Nb, Zr, and Y values (Table 1). Trace element contents of the garnet-biotite gneiss from Site 1137 are also presented in Table 1. Due to an instrumental fault, the low-mass values for the U. S. G. S. standard G-2 (granite) were not available to compare with the gneiss. Although the fault did not occur during the analysis of the gneiss, and a sample of the U. S. G. S. standard BHVO-1 (basalt) run at the same time compared very well to its certified values, we recommend that the low-mass values of the gneiss be considered cautiously.

Results of the PGE analyses for 17 Kerguelen basalt samples are presented in Table 1, along with 2 sigma errors calculated using the standard addition regression described by Ely and Neal (2001). Most 2 sigma values are between 5 and 40% of the analyzed value. Iridium values for the KP range from 0.30 to 0.97 ng/g, with many values falling between the limit of detection (LOD = background + 3σ) and the limit of quantification (LOQ = background + 10σ). The values for LOD and LOQ were calculated for each sample using the nearest background (blank) in the sample run. The rock concentration LOD for the PGEs was generally <0.4 ng/g (<1.3 pg/g analyzed concentration). Values are not included if they were within 3σ of background. Ranges for the other PGEs are as follows: Ru (0.28–1.56 ng/g), Rh (0.18–1.42 ng/g), Pt (5.8–32.6 ng/g), Pd (3.5–15.4 ng/g). As expected, the PGEs increase in concentration from Ir, Ru, Rh, to Pt. Palladium abundances are generally lower than for Pt (Table 1). Primitive mantle-normalized profiles show all samples have fractionated patterns with an overall positive slope, but generally exhibit a flattening of the profile between Pt and Pd and/or a positive Ir anomaly (Fig. 2).

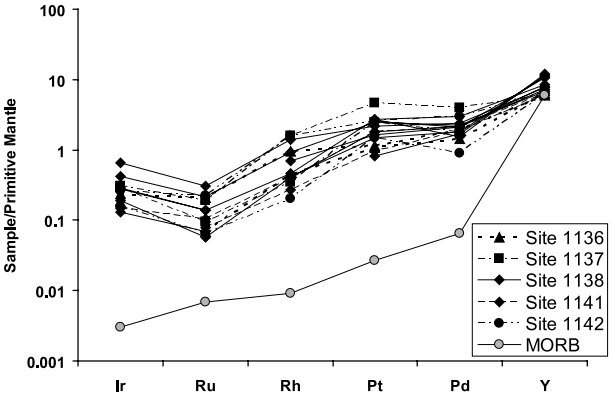

Fig. 2. Primitive mantle-normalized plot of the PGEs and Y from the Kerguelen Plateau. Nearly all samples show positive Ir anomalies, and exhibit a flattening of the profile between Pt and Pd. N-MORB data from Rehkämper et al. (1999) and Tatsumi et al. (1999). Primitive mantle values are from Sun and McDonough (1995).

6. DISCUSSION

6.1. Sulfide Effects

Petrographic observations demonstrate that sulfide mineral modal abundance is <<1% in all the Leg 183 samples examined in this study. This could be indicative of the following: 1) the basalts did not reach sulfide saturation; 2) the basalts did reach sulfur saturation and the resulting immiscible sulfide melt was effectively removed; 3) Sulfide was lost during subaerial or shallow water emplacement of the KP basalts (Moore and Schilling, 1973; Frey et al., 2000a); 4) most of the samples have also experienced at least mild seawater alteration when the KP became submerged, during which sulfides could have been removed (Keays and Scott, 1976).

There has been much discussion of the sulfur content of the mantle (e.g., Hart and Ravizza, 1996, and references therein). Estimates typically range from 20 μg/g for depleted mantle (Ionov et al., 1992) to 250 μg/g for primitive mantle (Keays, 1995). For modeling purposes, we will assume that plume source mantle material has 250 μg/g sulfur. When such a

source melts, the sulfide minerals that host the sulfur will be exhausted by a maximum of ~20%–23% partial melting (Rehkämper et al., 1999). We do note that Luguet et al., 2003, concluded that sulfides could be exhausted in oceanic mantle after only 12% partial melting, suggesting the 20%–23% partial melting represents an upper limit for sulfide exhaustion. At this level, all magmas generated by melting up to ~25% of an undepleted mantle source should be at or near saturation with sulfur. Other estimates, however, indicate that the capacity of the magma to incorporate sulfur is correlated negatively with pressure and positively with temperature, and that pressure has by far the greater effect (Mavrogenes and O'Neill, 1999; Holzheid and Grove, 2002) and this effect is nonlinear (see eqn. 10 of Mavrogenes and O'Neill, 1999). Therefore, the closer to the surface the magma gets, the greater its sulfur capacity. The KP and other LIPs are thought to be generated from melts of 20%–40% (Coffin and Eldholm, 1993; Mahoney et al., 1993; Farnetani et al., 1996; Neal et al., 1997); for modeling purposes we will assume ~30% melting. The pressure and temperature of the source during the melting of the KP was probably variable, but much of the melting likely took place at pressures between 2.0 and 3.0 GPa and temperatures in excess of 1400°C (see also Farnetani et al., 1996; Chazey and Neal, 2004; Fitton and Godard, 2004). Using these assumptions the model of Mavrogenes and O'Neill (1999) predicts a sulfur capacity of ~800–1060 μg/g for a basaltic magma. The Holzheid and Grove (2002) model predicts an even higher sulfur capacity (~1600 μg/g at ~1430°C and 2.0 GPa). Assuming a 30% melt of a KP source with 250 μg/g sulfur, the resultant magma will have 833 μg/g sulfur, and thus the initial melt would likely have been close to sulfur saturation.

If sulfur is not lost either due to sulfur saturation or as part of a gaseous phase, then it is likely almost perfectly incompatible during fractional crystallization. This allows an estimate to be made of the sulfur content of a magma provided the amount of fractional crystallization is known. Even if sulfur is not perfectly incompatible (i.e., $K_d = 0$), the approximation is useful because it provides a maximum sulfur concentration for the magma. If the maximum sulfur concentration is less than the saturation point, then sulfur cannot saturate without further crystal fractionation, a decrease in FeO or temperature, or an increase in pressure. Using the program "PELE" (Boudreau, 1999) a simple major element model was used to estimate the amount of fractional crystallization that the KP magmas underwent. If an experimentally derived ~30% partial melt of the natural, fertile spinel lherzolite KLB-1 (Hirose and Kushiro, 1993) is used as a primary melt, the KP basalts must have experienced no less than ~30% fractional crystallization of olivine (±spinel), plagioclase, and clinopyroxene. This would increase the sulfur content of the magma to ~1190 μg/g. Trace element modeling of the Site 1138 basalts by Neal et al. (2002) used 15% crystallization of plagioclase, clinopyroxene, and titanomagnetite with replenishment and resorption to produce the observed compositional ranges. Such crystallization increases sulfur content of the magma significantly. However, the higher sulfur content is offset by the increase in sulfur capacity caused by the magma's ascent into shallow, low-pressure magma chambers where most of the fractionation takes place. For example, a magma at 1400°C and 2.0 GPa would have a sulfur content at sulfide saturation (SCSS) of 1060 μg/g; when the ascending magma reached 1.0 GPa, the sulfur capacity (at 1400°C) of the magma would have increased to ~1400 μg/g (Eqn. 10; Mavrogenes and O'Neill, 1999, using the basaltic values for A [−6684 K], B [11.52], and C [−0.047 K bar^{-1}]), and at 0.1 GPa, 1800 μg/g. After 45% fractional crystallization, the sulfur concentration of the magma could be as much as ~1515 μg/g. We envisage the late stages of magma evolution are likely to have occurred in near-surface magma chambers at pressures between 1.0 and 0.1 GPa. However, the magma temperature during late-stage fractional crystallization (plagioclase, clinopyroxene) is likely to be under ~1200°C. The temperature drop would cause the SCSS to drop back to near ~1078 μg/g at 0.1 MPa. All these calculations, however, neglect the effects of magma composition. The most important compositional factor is FeO; the higher the FeO of a magma, the higher the SCSS (O'Neill and Mavrogenes, 2002). At low FeO, the other major element oxides do have an effect on the SCSS as well, but at ~10 wt % FeO, the effects of other oxides become inconsequential (O'Neill and Mavrogenes, 2002). As the Kerguelen basalts analyzed in this study all contain 11.5 wt % FeO or more, the effects of the other major elements can be treated as negligible. A strong exponential relationship between the SCSS and FeO content suggests that the SCSS for these magmas would be very high indeed. Estimates using the equations from O'Neill and Mavrogenes (2002) indicate that the SCSS may reach almost 7000 μg/g for the highest FeO abundance KP basalts. Given these high FeO abundances, it is very unlikely that the KP basalts could have saturated with respect to sulfur.

Wallrock interaction with either crustal or mantle material may change the sulfur concentration of the magma through assimilation, while decreasing its sulfur capacity due to the temperature decrease. Continental material typically has high concentrations of sulfur (697 μg/g; Wedepohl, 1995), and assimilation of such material may increase sulfur in the magma, while incorporation of depleted mantle sources would serve to decrease the sulfur through dilution. However, by the time the magma encounters continental material, it would have sulfur abundances far in excess of ~700 μg/g. The added fractionation associated with assimilation only serves to increase the natural sulfur abundance of the magma. In order for the sulfur not to be diluted in these cases, sulfide would have to be preferentially assimilated by the magma. Studies have shown this to be a strong possibility, as the high temperatures of the magma preferentially destabilize phases like pyrite in the wallrock (Barnes et al., 1997; Baker et al., 2001). Therefore, magmas with sulfur abundances greater than 700 μg/g may still be enriched in sulfur via wallrock assimilation.

If segregation of a sulfur-rich liquid had occurred, relatively large depletions of Pt and Pd relative to Y on primitive mantle normalized plots would be expected in the remaining silicate liquid (Brügmann et al., 1993). In a sulfide-undersaturated basaltic system, Pd and Y should have similar incompatibilities, producing a relatively flat normalized pattern [i.e., $(Y/Pd)_{pm}$ ~1)]. The PGE data for the KP basalts (Fig. 2) show a slight depletion of Pd [$(Y/Pd)_{pm}$ ranges from 1.5 to 13, whereas N-MORB is ~40)]. MORBs are generally considered to have experienced sulfide saturation and extraction of an immiscible sulfide melt (e.g., Roy-Barman et al., 1998; Rehkämper et al., 1999; Chazey, 2004). They plot well below the KP on a

Table 2. Model concentrations (ng/g) and crystal/liquid partition coefficients for the KP modeling.

		Ir	Ru	Rh	Pt	Pd	Reference[a]
Olivine	Kd	0.77	1.7	1.8	0.08	0.03	1, 11
Orthopyroxene	Kd	1.8	1.9	0.27	2.2	0.3	2
Clinopyroxene	Kd	1.8	1.9	0.27	0.8	0.3	3
Cr-spinel	Kd	100	151	63	3.3	1.6	4, 11
Sulfide	Kd	4400	2400	3000	6900	6300	5
Plagioclase	Kd	0.3	0.3	0.4	0.3	0.2	6
Ti-magnetite	Kd	500	300	130	3	1.1	7
Spinel Lherzolite	ng/g	2.46	4.29	0.8	4.34	2.48	8
Primitive Mantle	ng/g	3.2	5.0	0.9	7.1	3.9	9
Outer Core (Model 3)	ng/g	188	669	134	776	572	10
Outer Core (Model 4)	ng/g	332	1181	237	5254	3873	12

[a] References for data are as follows: 1 = Puchtel and Humayun (2001), Capobianco et al. (1991); 2 = estimates from Ely and Neal (2003), Rh estimated from Hill et al. (2000); 3 = Capobianco et al. (1990, 1991), Capobianco and Drake (1994), Hill et al. (2000); 4 = Puchtel and Humayun (2001), Capobianco et al. (1990); 5 = Peach et al. (1994), Bezmen et al. (1994), Tredoux et al. (1995); 6 = Capobianco et al. (1990, 1991), Capobianco and Drake (1994); 7 = Capobianco et al., 1994, estimates from Ely and Neal (2003); 8 = Rehkämper et al. (1997); 9 = McDonough and Sun (1995); 10 = Snow and Schmidt (1998); 11 = Righter et al. (2004); 12 = Brandon et al. (2003).

primitive mantle normalized plot (Fig. 2), and show extreme depletions of Pt and Pd relative to Y. Therefore, PGE data for the KP basalts indicate that the magma that produced them did not segregate an immiscible sulfide liquid. The slight depletions in Pd will be explained below.

The basalts of Sites 738 and 1137 and to some degree those of Site 1136 interacted with continental lithospheric material (Storey et al., 1992; Weis et al., 1993; Mahoney et al., 1995; Neal et al., 2002). While we did not analyze any basalts from Site 738, the overall PGE abundances of the basalts analyzed from Site 1136 and 1137 show no significant difference from KP basalts that do not contain continental components (Sites 1138, 1141, and 1142). The similarity between the PGE abundances at each of the sites suggests that although some basalts have been affected by assimilation of continental crust, this has not dramatically affected the PGEs either through dilution or through promoting sulfur saturation and removal of an immiscible S-rich liquid.

Finally, while the presence of vesicles in many KP basalts indicates the magmas lost volatiles via degassing, it is unlikely that this would affect PGE abundances due to the high volatility temperature of these elements. Seawater alteration could have removed sulfide minerals from the host basalts, but if so, the PGEs were incorporated into alteration phases and basalts retained their relative whole-rock abundances. Given the evidence based on petrography, sulfur saturation models, and PGE data, it is likely that the KP magmas did not saturate with respect to sulfur, and that the PGEs exhibited lithophile behavior during the evolution of the Kerguelen Plateau basalts.

6.2. PGE Behavior during Basalt Petrogenesis

At Site 1138, a sequence of subaerially erupted tholeiitic basalts was recovered that has been previously modeled by replenishment and fractional crystallization (Neal et al., 2002). Although the Site 1138 basalt compositions require earlier stages of crystallization that include olivine, the last stage to take place before eruption included plagioclase, clinopyroxene, and a small amount of titanomagnetite. By determining PGE abundances in the basalt units throughout the sequence, fractionation of the PGE profile can be monitored. This can be achieved using the Pt/Ir ratio. This ratio is useful as a fractionation index as Pt ranges from a bulk D of ~1 to being slightly incompatible during a typical fractionation sequence, while Ir remains compatible during the fractionation (see Table 2 for crystal/liquid partition coefficients). The Pt/Ir ratio for the Site 1138 basalts shows a general negative correlation with Cr, Sc, and Ni (Fig. 3), all of which are compatible in clinopyroxene and titanomagnetite (e.g., Villemant et al., 1981; Green, 1994). Conversely, the Pt/Ir ratio correlates positively with TiO_2 (Fig. 3c), and Cr exhibits a generally positive correlation with Ir (Fig. 3f). One of the samples falls off of the Pt/Ir vs. Cr trend (Sample 1138 80R5), but this may be due to a large error on Ir (0.6 ± 0.3 ng/g; instrument sensitivity was lower for this particular run). All of these plots show some variability in the degree of correlation, but that is consistent with the complexity of the RFC processes inferred to have affected these basalts (Neal et al., 2002). Although plagioclase was fractionating, a positive correlation between Pt/Ir and Eu (Fig. 3d) suggests that Eu was behaving incompatibly overall. This is consistent with the conclusion of Neal et al. (2002) that the amount of plagioclase crystallization was not enough for the bulk K_d of Eu to exceed unity. While there is also a possibility that the PGEs may be present as metal alloys (e.g., Ballhaus and Sylvester, 2000), in the KP basalts, the presence of titanomagnetite as a fractionating phase suggests fO_2 was too high for such alloys to form (e.g., Barnes, 1993; Tredoux et al., 1995; Borisov and Palme, 1997; Ertel et al., 1999).

As stated earlier, the presence of Cr-spinel in Sites 1141 and 1142 basalts correlates strongly with whole-rock Cr contents of these basalts (Table 1). According to the partition coefficients used in our modeling (see below and Table 2), the PGEs should be affected in much the same way. If the increase between the low (tholeiitic) and high (alkalic)-Cr samples is between 3 and 40 times, we could reasonably expect to see an appreciable increase in Ir and Ru. Spinel-melt partition coefficients for Cr (~200; Puchtel and Humayun, 2001) are not much higher than Ir and Ru and at the very least, we might expect a two-fold increase in PGE contents in the samples. However, this is not the case. The basalts at Sites 1141 and 1142, Unit 1 have comparable PGE concentrations to the Site 1136 and 1138

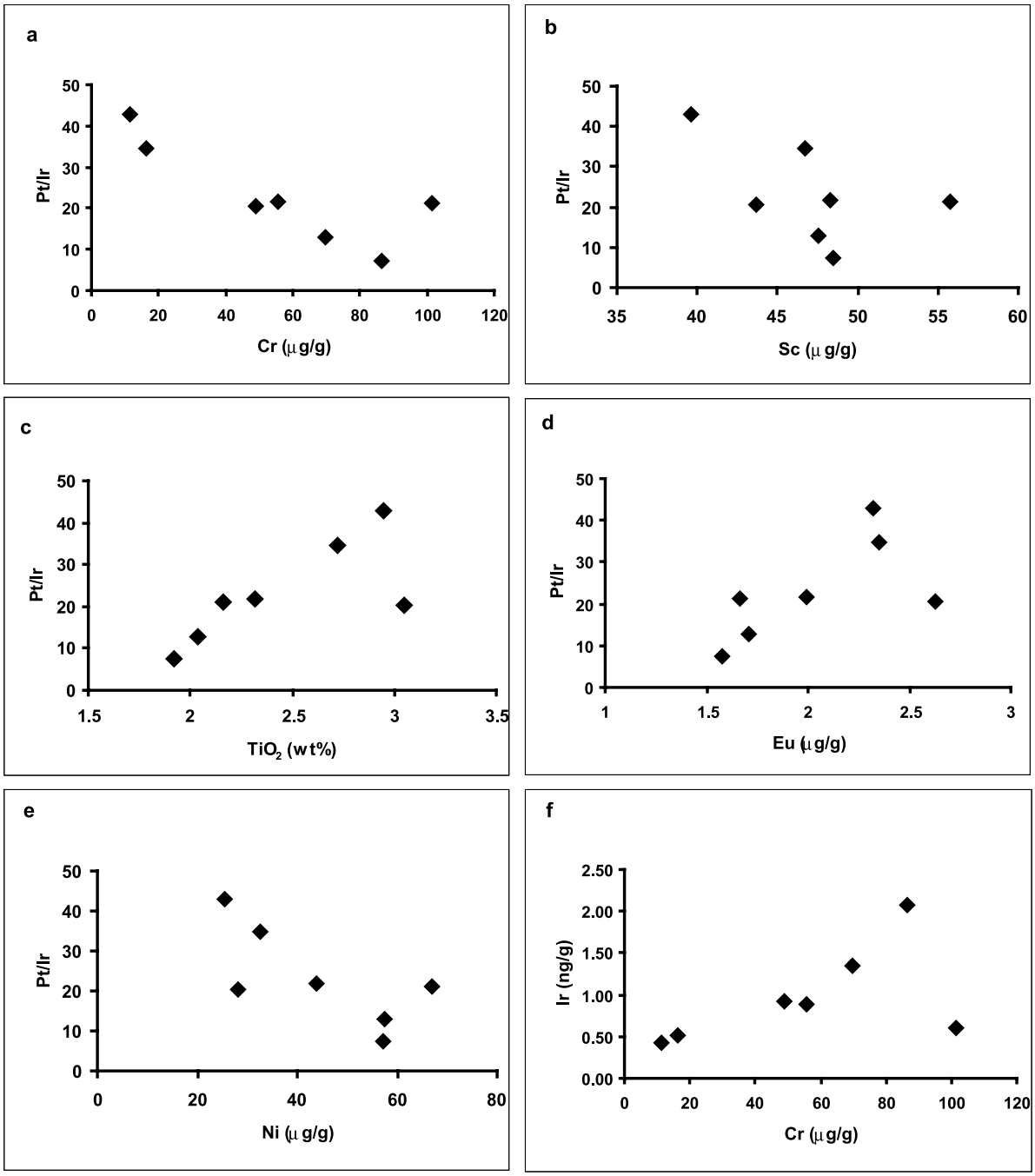

Fig. 3. Fractional crystallization indicators compared with Pt/Ir and Ir abundance for Site 1138 basalts. Positive correlation of Pt/Ir with TiO_2 (c) and Cr with Ir (f), and negative correlations of Pt/Ir with Cr, Sc, Eu and Ni (a, b, d, and e) indicate Pt and Ir are in a sulfur-undersaturated environment, such that Pt has a bulk partition coefficient around one and Ir is compatible in a fractionating phase. Pt/Ir correlation with Cr and Sc coupled with a negative correlation with TiO_2 may suggest clinopyroxene and titanomagnetite are responsible for the compatible behavior of Ir. This is in agreement with the K_ds in the literature (Table 2).

basalts. But they also formed from a lower degree of partial melting than those at Sites 1136 and 1138 (Neal et al., 2002). This model predicts that a lower degree of partial melting would decrease the concentration of Ir and Ru in the primary magma. This would result in decreased overall Ir and Ru abundances relative to other samples, provided that a similar amount of the same phases were crystallized from their parent melts. The presence of Cr-spinel could therefore act as a counterbalance to the lower abundance of PGE abundance in the primary magma to the Site 1141 and 1142 alkalic basalts, and thus the final basalt. In other words, the Cr-spinel crystals bring up what would otherwise be lower PGE abundances in the Site 1141 and 1142 alkalic basalts.

On the larger scale, the KP basalts mark a change in trend

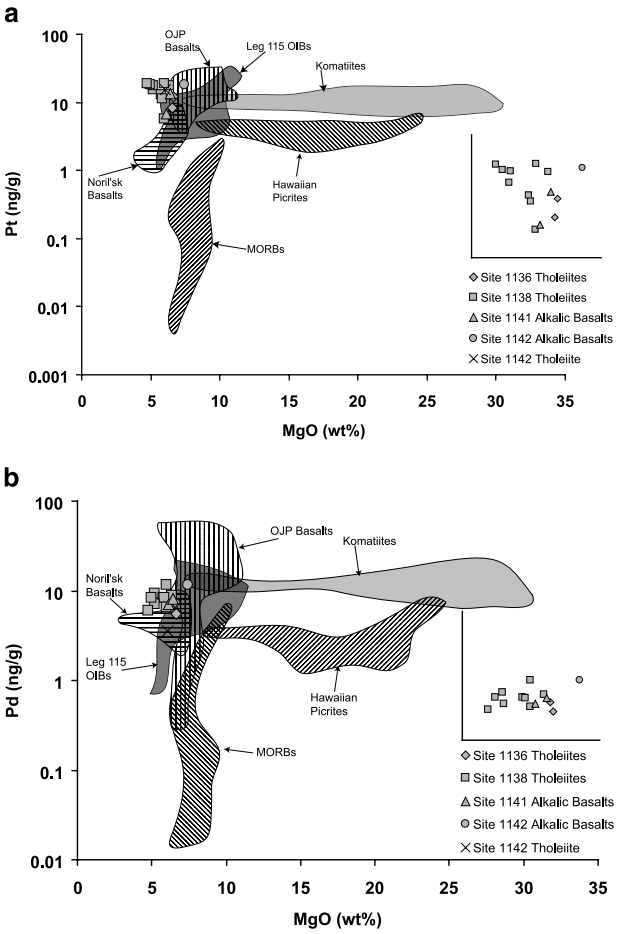

Fig. 4. Pt and Pd (ng/g) vs. MgO (wt%) for the KP basalts compared with various other types of basalts, picrites, and komatiites. The insets in each figure display only the KP data. (a) Sulfur undersaturated systems like the Baltic komatiites (Vetreny) and the KP basalts indicate Pt has a bulk partition coefficient near one during olivine and Cr-spinel fractionation. The bulk partition coefficient decreases after olivine and Cr-spinel move off the liquidus. MORBs are likely affected by sulfide saturation. (b) Again, sulfur undersaturated systems reflect the incompatible behavior of Pd during olivine and Cr-spinel fractionation. However, Pd abundances in the KP basalts decrease with decreasing MgO abundance during fractionation of plagioclase, clinopyroxene and titanomagnetite. This behavior is inconsistent with current K_ds for Pd, and combined with other evidence (see text) is indicative of Pd removal by secondary alteration processes. Data are from Arndt and Nesbitt (1984), Arndt (1986), Lightfoot et al. (1990), Fryer and Greenough (1992), Brügmann et al. (1993), Devey et al. (1994), Puchtel et al. (1996), Norman and Garcia (1999), Rehkämper et al. (1999), Tatsumi et al. (1999), Bennett et al. (2000), Puchtel and Humayun (2001), Tejada et al. (1996, 2002), Ely and Neal (2003), Chazey and Neal (2004), Fitton and Godard (2004).

relative to komatiites and picrites on MgO vs. Pt and Pd diagrams (Figs. 4a,b). From the komatiite field, Pt in a sulfur-undersaturated system has a K_d of about one during olivine and Cr-spinel fractionation. This is consistent with published K_ds for the Pt in these phases (Table 2; Puchtel and Humayun, 2001). At or near the point at which olivine and Cr-spinel are no longer liquidus phases, it seems that MORB magmas experience sulfide saturation and removal of Pt (and the other PGEs), whereas the basalts from the KP and several from the OJP (Chazey and Neal, 2004) suggest Pt becomes slightly incompatible at this point, again consistent with published partition coefficients (Table 2). It is expected Pd would follow a similar trend, increasing with decreasing MgO, if a bit steeper due to Pd being more incompatible than Pt in silicate and oxide phases (Table 2; Puchtel and Humayun, 2001; Ely and Neal, 2003). For the Vetreny (komatiite) samples, this is true; the slope of the Pd trend is ~50% greater than that of Pt (Fig. 4b). However, the KP basalts show constant Pd values or a general decrease of Pd with MgO, appearing to behave in the opposite sense (i.e., it is compatible—see insets to Fig. 4) to Pt. On the basis of known partition coefficients, it is unlikely that the trend in Pd vs. MgO displayed by the KP basalts is a result of sudden increased compatibility. Furthermore, this cannot be an effect of sulfide removal because such a process would have affected all the PGEs, not just Pd (e.g. Bezmen et al., 1994), and Pt clearly does not follow the same trend (Fig. 4a).

Studies around PGE ore bodies have demonstrated that Pd is more mobile than Pt in surficial (low temperature) environments and is transported in solution (e.g., Wood and Vlassopoulos, 1990). Previously, Barnes et al. (1985) concluded that hydrothermal alteration preferentially mobilized Pd relative to the other PGEs. Studies have also demonstrated that this enhanced low-temperature Pd mobility is independent of climate (e.g., Taufen and Marchetto, 1989; Prichard and Lord, 1990; Salpeteur and Jezequel, 1992). This behavior of Pd has been quantified by experimental work (e.g., Wood, 1990; Bowles et al., 1994). Therefore, as with basalts from the Ontong Java Plateau (Ely and Neal, 2003), we suggest that the Pd abundances of the KP basalts have been affected by low temperature alteration processes (Wood and Vlassopoulos, 1990). Thus, the flattening of the primitive mantle-normalized pattern from Pt to Pd (Fig. 2) is an artifact of secondary alteration (Ely and Neal, 2003). This also explains why the Y/Pd values are slightly increased over primitive mantle in the KP basalts, without evidence for sulfur saturation and sulfide segregation.

6.3. Site 1137

The two samples from Site 1137, the Unit 2B tholeiitic basalt, which on the basis of isotopic data contains a component of continental crust (Weis et al., 2001), and the garnet-biotite gneiss cobble, have PGE concentrations that fall within error of the rest of KP basalts. Continental crust is known to have low PGE abundances (Wedepohl, 1995; Gao et al., 1998). On the basis of current knowledge, it is unlikely that the PGEs would be compatible in any of the minerals in the gneiss except for magnetite (Table 2; see Mitchell and Keays, 1981, for PGEs in garnet, and Capobianco et al., 1991, and Capobianco and Drake, 1994, for PGEs in plagioclase feldspar; no data are available for PGEs in K-feldspar and quartz, although we assume such contents in these minerals would be low). If the few percent of magnetite were responsible for the relatively high PGE abundances, a roughly negatively sloped primitive mantle-normalized PGE pattern would result. However, Rb, Nd, and Pb isotopes indicate that these gneisses are very similar to Domain 2 of the Eastern Ghats in India (Ingle et al., 2002). In addition, U-Pb dates from zircons and monazites in the garnet-biotite gneiss clast have a similar age range to those of zircons in the Eastern Ghats (Nicolaysen et al., 2001). The

Table 3. Source mineralogy and melting proportions for the KP modeling.

	Garnet lherzolite	Spinel lherzolite	Stage 1	Stage 2	Stage 3	Stage 4
Olivine	0.6000	0.6000	0.371	0.313	0.45	0.425
Orthopyroxene	0.1500	0.1500	0.200	0.150	0.25	0.250
Clinopyroxene	0.1994	0.1994	0.275	0.200	0.30	0.325
Cr-spinel	0.0000	0.0500	0.000	0.333	0.00	0.000
Sulfide	0.0006	0.0006	0.004	0.004	0.00	0.000
Garnet	0.0500	0.0000	0.150	0.000	0.00	0.000

protolith of the Eastern Ghats granulites may be a tholeiitic basalt, possibly produced by a plume in a rift environment (Subba and Divakara, 1999). In this case, plume-derived basalts could be responsible for the PGEs in the garnet-biotite gneiss, with the implication that the PGEs are relatively immobile during metamorphism. Ingle et al. (2002) indicated, however, that the Pb isotopes of the gneiss are those of ancient continental material. These authors also suggested that sandstones in the conglomerate housing the gneiss clasts have isotopic signatures supporting mixing between the gneiss and younger tholeiitic basalt flows. In this second case, addition of PGEs to the gneiss via metasomatism is the most likely mechanism, where the gneiss must have interacted with the pre-Kerguelen tholeiitic magma now represented in the sandstone and/or the Kerguelen plume itself. In either case, the Kerguelen plume would be the source for the PGEs.

6.4. Modeling of the KP Basalt PGE Compositions

6.4.1. Modeling Parameters

Partition coefficients for the PGEs were acquired from literature sources where possible. In cases where a range of partition coefficients was given (e.g., Capobianco and Drake, 1994), the K_d was chosen to best fit the data. At this time, orthopyroxene partition coefficients are not available and were assumed for the sake of the model to be the same as for clinopyroxene (as was done by Ely and Neal, 2003, for the modeling of the OJP basalt PGEs). Source mineralogy and mineral-melt proportions were adapted from Ely and Neal (2003) and are presented in Table 3. In our modeling, we use three mantle sources: 1) depleted mantle; 2) primitive mantle; 3) primitive mantle containing up to 1% of an outer core component. In the first model, the "average spinel lherzolite" composition from Rehkämper et al. (1997) was chosen to represent an upper (depleted) mantle source. As no Rh value is reported for these samples, we estimated a value that would create a relatively smooth primitive mantle-normalized pattern. The second model utilizes the primitive mantle composition of McDonough and Sun (1995). The third model uses the same primitive mantle composition as in the second model along with up to 1% of an outer core component (Snow and Schmidt, 1998). Modeling the abundances of the PGEs during crystal fractionation was undertaken as described above.

6.4.2. Partial Melting and Fractional Crystallization

The KP basalts have relatively high levels of PGEs compared to other common basalts, such as ocean island basalts (OIBs; e.g., Fryer and Greenough, 1992) and MORBs (e.g., Devey et al., 1994; Rehkämper et al., 1999; Tatsumi et al., 1999), but have similar concentrations to other LIP basalts, such as those from the OJP (e.g., Ely and Neal, 2003; Chazey and Neal, 2004). Total PGE abundances for the KP basalts are roughly similar to some komatiites (e.g., Arndt and Nesbitt, 1984; Arndt, 1986; Brügmann et al., 1987; Puchtel and Humayun, 2001). Normalized Ir values are high relative to Ru and the overall PGE patterns are not as fractionated as expected given the extensive fractional crystallization that occurred to produce these basalts (indicated by relatively low MgO abundances).

To constrain the amount of partial melting and fractional crystallization that took place to produce the KP basalts, a model was constructed using nonmodal batch melting of a garnet lherzolite to 10%. This lherzolite then moved through the garnet-spinel transition and melted approximately a further 20%, for up to 30% partial melting of the rising plume source. Both sulfide and spinel were modeled to exhaust at 15% partial melting. The amount of garnet in the source is difficult to gauge, although the volume of the KP makes it unlikely that melting was restricted to the spinel stability field (cf. Coffin and Eldholm, 1993). The Zr/Y values of the KP increase with decreasing age of the plateau as a result of the lower degrees of partial melting at Sites 1141 and 1142 than those at Sites 1136 and 1138. It is unclear, however, whether the increased Zr/Y requires the presence of garnet in the source. Frey et al. (2000b) indicates that at least late stage Kerguelen Archipelago basalts have equilibrated with garnet, while those in the Ninetyeast ridge did not due to their proximity to the SEIR and consequent lower pressure of melting. Regardless, the PGEs are thought to be highly incompatible in garnet (Mitchell and Keays, 1981), and would not significantly fractionate the normalized PGE profile.

To generate the KP basalts, a two-stage crystallization sequence was employed. The first stage was based on PELE model calculations using a 28.9% melt of spinel lherzolite KLB-1 as the initial (primary) melt composition. [Note that the first 10% partial melting of KLB-1 was conducted in the garnet stability field by assuming all spinel was garnet; the remainder of the melting occurred in the spinel stability field.] This method is a first-order approximation of the crystallization sequence; any further complication to the model is unwarranted as no samples of early cumulate stages of crystallization were recovered. Varying some of the parameters resulted in small changes in the sequence, but most reasonable estimates suggest that the KP basalts have experienced between 30 and 50% fractional crystallization, with between 20 and 25% olivine fractionation. This amount of olivine fractionation produced

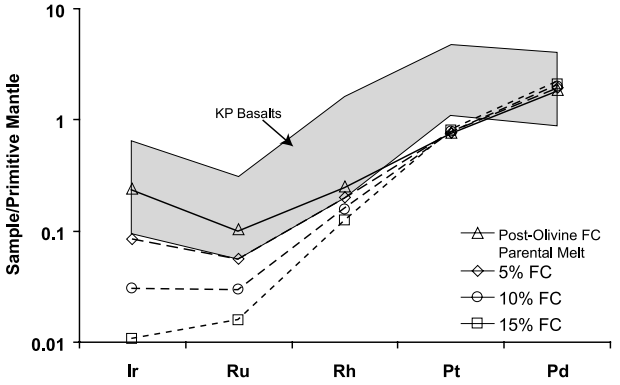

Fig. 5. Modeling of the KP basalts using nonmodal batch melting of a depleted upper mantle (spinel lherzolite) source. Spinel lherzolite data from Rehkämper et al. (1997). The "parental melt" is the concentration of the PGEs in the magma after olivine plus Cr-spinel fractionation (30%, 49:1), and the subsequent percentages indicate fractional crystallization of plagioclase, clinopyroxene, and titanomagnetite (15:9:1) after Neal et al. (2002). The gray field represents the range of KP basalt compositions.

magmas with ~8–9 wt% MgO, which was at the upper end of the range defined by KP basalts analyzed in this study. Spinel crystallization in the models varied from <1% to almost 4%. Plagioclase and clinopyroxene usually became saturated at almost the same time, typically fractionating more plagioclase than clinopyroxene. Total abundance of these two phases ranged from 10%–25% by mass. As the MgO content of KLB-1 is low relative to other spinel lherzolites, using this composition provides a lower limit with regard to the amount of olivine fractionation required. For our modeling purposes, parameters were adjusted slightly based on both physical and chemical observations and previous work (Neal et al., 2002). The MgO contents of the KP basalts require more olivine and/or clinopyroxene fractionation to occur than in the PELE models of the melt derived from KLB-1. As such, the first stage used in our model is 30% crystallization of olivine (98%) and Cr-spinel (2%). The second stage of crystallization is adapted from Neal et al. (2002) and involves 15% crystallization of 60% cpx, 36% plagioclase, and 4% titanomagnetite. The petrography supports this model (Neal et al., 2002). As noted above, samples from Site 1141 the uppermost unit of Site 1142 contain altered, partially resorbed olivine crystals and small Cr-spinel crystals, indicating that while no longer stable, these phases were crystallizing at one point. Primary Cr-spinel crystals are only present in these samples when protected by an encapsulating olivine crystal, suggesting any and all other spinel crystals have been resorbed. The Cr abundances of these three samples (300–405 μg/g) are much higher than the other KP samples analyzed in this study (11–101 μg/g) The PELE modeling supports these observations, as in all cases spinel moves off of the liquidus before plagioclase and clinopyroxene precipitate.

6.4.3. Model 1

The spinel lherzolite source contains insufficient PGEs to produce the KP basalt compositions via partial melting followed by fractional crystallization of the resulting magma (Fig. 5). Given the fractional crystallization requirements from the MgO content of these basalts, the magmas that produced the KP basalts experienced close to 45% total crystallization. Therefore, the model significantly underestimates the amount of Ir, Ru, Rh, and Pt. Although this model can account for the lowest Pd abundance of the KP basalts, these are not true magmatic abundances because Pd was lost during low-temperature alteration. Ely and Neal (2003) demonstrated that it was possible to preferentially remove more than half the primary Pd abundance by such low-temperature alteration (see their fig. 1). Subsequent stages of replenishment and fractional crystallization, as invoked by Neal et al. (2002), serve to flatten the overall PGE profile (based on the partition coefficients for magnetite reported by Capobianco et al., 1991, and Capobianco and Drake, 1994), requiring more fractional crystallization to counter this. Adding several replenishments to the system does not alter the overall outcome of this model, which indicates that the KP source must have contained PGE abundances higher than those in depleted upper mantle.

It is important to note that this and all subsequent models produce the positive Ir anomaly seen in the KP basalts. The use of the K_ds for Ir and Ru for Cr-spinel from Puchtel and Humayun (2001) are largely responsible for this effect. The more recent study of Righter et al. (2004), which included experimental determination of the partition coefficients of Ir and Ru into spinel, does not resolve the anomaly issue. Their results indicate that the $K_d^{spinel/melt}$ for Ir and Ru range from 5 to 22,000 and 76 to 1143, respectively. Again, depending on which values are chosen, model reproduction of PGE patterns both with and without Ir anomalies are possible. Preferential resorption of titanomagnetite may also produce this pattern.

6.4.4. Model 2

The second model uses a primitive mantle source and the same melting-crystallization parameters as in Model 1 (Table 3). Although the predicted PGE abundances are higher than that of our depleted mantle source model, it again fails to produce all of the PGE concentrations in the KP basalts (Fig. 6). The resulting abundances for Ir, Ru, and Rh are still an order of magnitude too low, though the modeled Pt and Pd are in the range of the KP basalts. As neither the depleted upper mantle nor the primitive mantle can produce the PGE concentrations in the KP basalts, it appears that the plume source must have contained some other PGE-rich component. We have already demonstrated that assimilation of continental crust did not affect the PGE abundances in the Site 1136 and 1137 basalts. This PGE excess in the mantle, relative to what there should be assuming efficient metallic core segregation, could be a result of the addition of a meteoritic late veneer of PGEs to the Earth after core formation, which is subsequently mixed into the mantle (e.g., Morgan, 1986). However, the primitive mantle estimates of McDonough and Sun (1995) already include this feature. We therefore suggest that an outer core component was included in the KP plume source.

6.4.5. Model 3

If LIPs are plume-generated, the large size of some of them requires an origin at the core-mantle boundary (e.g., Griffiths and Campbell, 1990; Coffin and Eldholm, 1993, 1994). Models

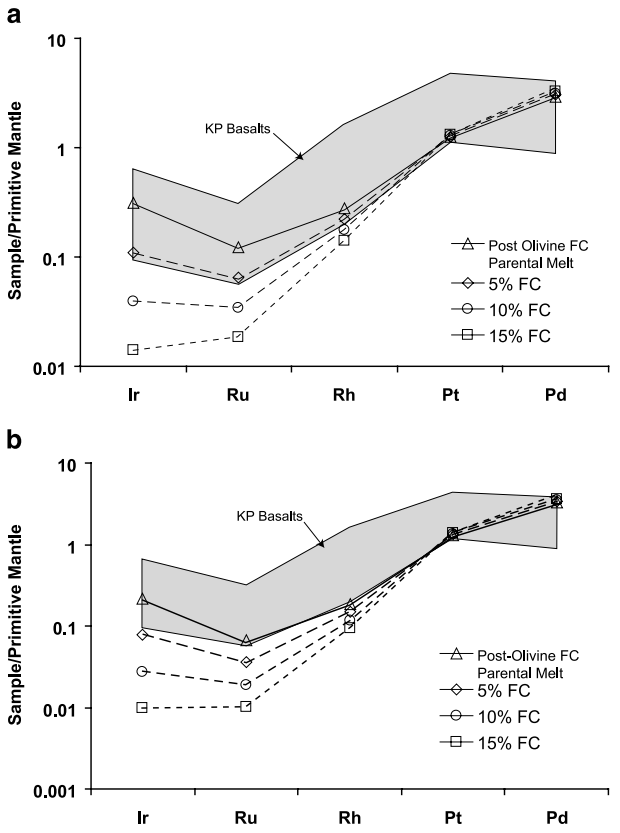

Fig. 6. (a) Modeling of the KP basalts using nonmodal batch melting of a primitive mantle source (McDonough and Sun, 1995). The parameters are otherwise identical to those in Figure 5. The gray field represents the range of KP basalt compositions. Again the model fails to account for KP basalts with the highest PGE abundances. (b) Model of the KP basalts using the same parameters as Figure 5, but including the RFC process of Neal et al. (2002). The parental melt is the magma generated by replenishment of 5% by weight of the primary magma, with 8% magma escape, and 0.2% resorption after 15% of the original (3rd overall stage) magma crystallized. Subsequent fractionation of the assemblage plagioclase, clinopyroxene, and titanomagnetite would represent a third stage. The parental melt approaches the pattern but not the abundance of PGEs necessary to produce the KP basalts.

for plume-derived magmas have used geochemistry as evidence for such an interaction (Walker et al., 1995, 1997; Brandon et al., 1999; Ely and Neal, 2003; Chazey and Neal, 2004). Geophysical evidence suggests the presence of partial melts, convection, and strong physical heterogeneity at the D" layer (e.g., Vidale et al., 1998; Vinnik et al., 1998). Experimental studies indicate that percolation of the liquid outer core into the base of the mantle is possible (Shannon and Agee, 1998), such that the outer core may influence the composition of a mantle plume at its source.

While we note that estimates for the amount of PGEs in the outer core are also model dependent, the available estimates (Table 2; Snow and Schmidt, 1998) illustrate the dramatic effect adding only a small amount of outer core to a plume source can have on the PGE contents in the derived basalts. The outer core material was "added" to primitive mantle by assuming 1% (for example) by weight core material metasomatized the plume source. The PGE abundances of the source material were then recalculated as a weighted average of plume and core. Figures 7a,b show the effect of addition of 0.3 and 1% of outer core material, respectively, to the primitive mantle source. However, the magma generated by 15% fractional crystallization contains Ir and Ru abundances that are below the range of the KP basalts, but 15% is required by the modeling of the other trace elements (Neal et al., 2002). Including up to

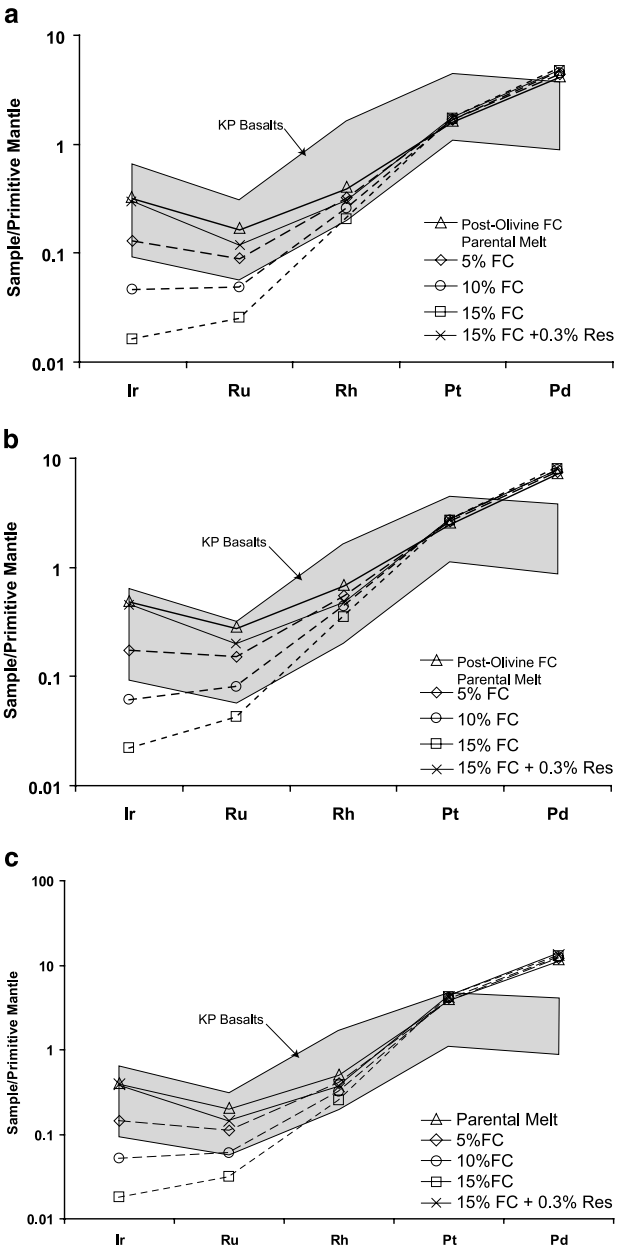

Fig. 7. Modeling of the KP basalts using nonmodal batch melting of a primitive mantle source (McDonough and Sun, 1995) metasomatized by (a) 0.3% and (b) 1% outer core material from Snow and Schmidt (1998). (c) uses the same parameters as that of (a), but applies the outer core values generated from Brandon et al. (2003). The gray fields represent the range of KP basalt compositions. Also plotted on each figure are compositions resulting from 15% fractional crystallization (as in Fig. 5) and 0.3% resorption of 1:3:6 olivine, clinopyroxene and titanomagnetite. Varying the degree of fractional crystallization, replenishment, and resorption presumed experienced by this PGE-enriched primary melt can reproduce the full range of the KP basalts.

0.3% resorption of an olivine, clinopyroxene, and titanomagnetite cumulate (in the proportions 1:3:6) generates the range of abundances shown in Figures 7a,b and reported in Table 1.

6.4.6. Model 4

While the Snow and Schmidt (1998) estimate is the only one available that predicts abundances for all of the PGEs in the earth's outer core, more recent models (Brandon et al., 2003) indicate that the core may have crystallized over a longer period than that used by Snow and Schmidt. The Snow and Schmidt model assumes the core has crystallized instantaneously at 4.5 Ga, whereas the four models presented in Brandon et al. (2003) assume that at least some crystallization is still occurring today. To apply the new core data to the KP models, we first had to select a core crystallization model from Brandon et al. (2003). These authors indicated that either their model 3 (constant crystallization of the core starting at 4.3 Ga) or model 4 [delayed start to crystallization of the core (3.5 Ga) followed by an intermediate rate of cooling] best fit their data. In all cases, including the model of Snow and Schmidt, crystallization of the core progresses to 5.5 weight % of the Earth. We have chosen to apply model 4 of Brandon et al. (2003) to the KP basalts.

As the models presented in Brandon et al. (2003) only supply information on Pt, Re, and Os abundances, the remaining PGEs had to be estimated from these values. Osmium and Ir are of similar abundance in the Snow and Schmidt (1998) model (176 and 188 ng/g, respectively) and we therefore chose to use the Os value from Brandon et al. (2003) as representative of the Ir abundance. The Pd abundance was acquired by assuming that the ratio of Pt to Pd in the Brandon et al. (2003) model would be the same of that as Snow and Schmidt (1998). The Ru and Rh abundances were calculated assuming the ratios of Ir to Ru and Rh were also the same as that for Snow and Schmidt (1998). The new values for outer core are presented in Table 2. Platinum and Pd abundances are ~7 times higher than the Snow and Schmidt (1998) model, while those of Ir, Ru, and Rh, are approximately twice as high.

Other than these new PGE abundances for outer core, our Model 4 uses the same parameters as those of Model 3. All of the PGE abundances for outer core used in Model 4 are significantly higher than those used for Model 3, such that only 0.3% outer core is necessary to produce the Pt and Pd values of the KP (Fig. 7c). However, although Pt and Pd are modeled successfully with only 0.3% outer core, the Ir, Ru, and Rh fall short of the uppermost KP PGE abundances. This could be remedied either by decreasing the amount of Cr-spinel and titanomagnetite that fractionally crystallize in the model, or by choosing slightly lower partition coefficients for Ir, Ru, and Rh in Cr-spinel and titanomagnetite. Both of these options increase Ir, Ru, and Rh relative to Pt and Pd, allowing for Model 4 to successfully account for PGE abundances in the KP.

7. CONCLUSIONS

The Kerguelen Plateau basalts from ODP Leg 183 have PGE abundances similar to those of komatiites and other LIPs, such as the Ontong Java Plateau. These relatively high abundances are not the result of sulfide accumulation, as deduced from petrography, lithophile/chalcophile element ratios, and geochemical modeling. While sulfide loss via alteration is a possibility, it is unlikely because removal of sulfide would also remove a significant portion of the PGEs. Sulfur saturation models, when applied to the KP basalts, suggest that the magma never became sulfur saturated and therefore never segregated an immiscible sulfide melt during its ascent. The high temperatures, high FeO abundances, and decreasing pressures associated with the rising Kerguelen plume combine to keep the sulfide capacity of the magma high enough to prevent sulfur saturation despite the extensive fractional crystallization experienced by the KP basalts. Using an experimentally determined melt composition and PELE modeling as a basis for a first-order approximation, a two-stage fractionation regime was developed for the KP basalts. The first involved 30% olivine plus Cr-spinel fractionation (49:1), and a second stage using a replenishment and fractional crystallization (RFC) model that included clinopyroxene, plagioclase, and titanomagnetite (15:9:1) (cf. Neal et al., 2002).

The PGE patterns of the KP basalts are reproducible although we note that this is dependent upon certain modeling parameters. What cannot be produced via petrogenetic modeling is the flat transition from Pt to Pd on primitive mantle-normalized plots. This coupled with a lack of correlation with any fractionation indices leads to the conclusion that Pd has been preferentially mobilized during secondary alteration. The positive Ir anomaly is a result of it having a lower bulk D than Ru during olivine + Cr-spinel crystallization, while the variation in the Ir anomaly may also be due in part to crystallization and resorption of titanomagnetite later during magma evolution. While the PGE patterns can be reproduced using models that involve melts originating in both depleted and fertile mantle sources, neither can account for the overall PGE abundances in the KP basalts, which require a source that is enriched in the PGEs above the concentrations in primitive mantle. On the basis of current estimates of PGE partition coefficients, the PGE abundances in the KP basalts are consistent with a primitive mantle source enriched with up to 1% of outer core material as defined by Snow and Schmidt (1998). Alternatively, 0.3% outer core material is sufficient if model 4 from Brandon et al. (2003) is used to calculate the outer core PGE abundances.

Acknowledgments—We are deeply indebted to the officers and crew of the R. V. *JOIDES Resolution* for the help and professionalism in obtaining drill cores during ODP Leg 192. We would like to thank Mike Rhodes and his group for the major element analyses. The ODP is sponsored by the US National Science Foundation (NSF) and participating countries under the management of Joint Oceanographic Institutions (JOI), Inc. Funding for this research was provided by grants from the United States Science Support Program to CRN. Thank you also to Dr. John Lassiter and Dr. Olivier Alard for reviews to an earlier version of this paper, and to 3 anonymous reviewers of the current version. The time and effort put in by the reviewers has greatly improved this paper.

Associate editor: A. Brandon

REFERENCES

Arndt N. T. and Nesbitt R. W. (1984) Magma mixing in komatiitic lavas from Munro Township, Ontario. In *Archaen Geochemistry* (ed. A. Kŕoner et al.), pp. 99–114. Springer-Verlag, Berlin.

Arndt N. T. (1986) Differentiation of komatiite flows. *J. Petrol.* **27,** 279–301.

Baker D. R., Barnes S.-J., Simon G., and Bernier F. (2001) Fluid transport of sulfur and metals between sulfide melt and basaltic melt. *Can. Min.* **39,** 537–546.

Ballhaus C. and Sylvester P. (2000) Noble metal enrichment processes in the Merensky Reed, Bushveld Complex. *J. Petrol.* **41,** 545–561.

Barling J., Goldstein S. L., and Nicholls I. A. (1994) Geochemistry of Heard Island (Southern Indian Ocean): Characterization of an enriched mantle component and implications for enrichment of the sub–Indian Ocean mantle. *J. Petrol.* **35,** 1017–1053.

Barnes S. J. (1993) Partitioning of the platinum-group elements and gold between silicate and sulphide magmas in the Munni Munni Complex, Western Australia. *Geochim. Cosmochim. Acta* **57,** 1277–1290.

Barnes S. J., Naldrett A. J., and Gorton M. P. (1985) The origin of the fractionation of platinum-group elements in terrestrial magmas. *Chem. Geol.* **53,** 303–323.

Barnes S.-J., Zientek M. L., and Severs en M. J. (1997) Ni, Cu, Au and platinum-group element contents of sulphides associated with intraplate magmatism. *Can. J. Earth. Sci.* **34,** 337–351.

Bennett V. C., Norman M. D., and Garcia M. O. (2000) Rhenium and platinum group element abundances correlated with mantle source components in Hawaiian picrites: Sulphides in the plume. *Earth Planet. Sci. Lett.* **183,** 513–526.

Bezmen N. I., Asif M., Brügmann G. E., Romanenko I. M., and Naldrett A. J. (1994) Distribution of Pd, Rh, Ru, Ir, Os and Au between sulfide and silicate melts. *Geochim. Cosmochim. Acta* **58,** 1251–1260.

Birkhold A. (2000) A geochemical investigation of San Cristobal (Makira) basement: Evidence for the presence of Ontong Java Plateau crust. Ph.D. thesis. University of Notre Dame.

Borisov A. and Palme H. (1997) Experimental determination of the solubility of platinum in silicate melts. *Geochim. Cosmochim. Acta* **61,** 4349–4357.

Boudreau A. E. (1999) PELE—A version of the MELTS software program for the PC platform. *Comp. Geosci*. **25,** 201–203.

Bowles J. F. W., Gize A. P., Vaughan D. J., and Norris S. J. (1994) Development of platinum-group minerals in laterites—Initial comparison of organic and inorganic controls. *Trans. Instn. Min. Metall. Sect. B Appl. Earth Sci.* **103,** B53–B56.

Brandon A. D., Norman M. D., Walker R. J., and Morgan J. W. (1999) ^{186}Os-^{187}Os systematics of Hawaiian picrites. *Earth Planet. Sci. Lett.* **174,** 25–42.

Brandon A. D., Walker R. J., Puchtel I. S., Becker H., Humayun M., and Revillon S. (2003) ^{186}Os-^{187}Os systematics of Gorgona Island komatiites: Implications for early growth of the inner core. *Earth Planet. Sci. Lett.* **206,** 411–426.

Brügmann G. E., Arndt N. T., Hofmann A. W., and Tobschall H. J. (1987) Noble metal abundances in komatiite suites from Alexo, Ontario and Gorgona Island, Colombia. *Geochim. Cosmochim. Acta* **51,** 2159–2169.

Brügmann G. E., Naldrett A. J., Asif M., Lightfoot P. C., Gorbachev N. S., and Ferorenko V. A. (1993) Siderophile and chalcophile metals as tracers of the evolution of the Siberian Trap in the Noril'sk region, Russia. *Geochim. Cosmochim. Acta* **57,** 2001–2018.

Campbell I. H. and Griffiths R. W. (1990) Implications of mantle plume structure for the evolution of of flood basalts. *Earth Planet. Sci. Lett.* **99,** 79–93.

Capobianco C. J., Drake M. J., and Rogers P. S. Z. (1990) Experimental solubilities and partitioning behavior of noble metals among lithophile magmatic phases. *Proc. Lunar Planet. Sci. Conf.* **21,** 166–167.

Capobianco C. J., Drake M. J., and Rogers P. S. Z. (1991) Crystal/melt partitioning of Ru, Rh and Pd for silicate and oxide basaltic liquidus phases. *Proc. Lunar Planet. Sci. Conf.* **22,** 179–180.

Capobianco C. J. and Drake M. J. (1994) Partitioning and solubility of PGEs in oxides and silicates. *Min. Mag.* **58A**, 144–145.

Capobianco C. J., Hervig R. L., and Drake M. J. (1994) Experiments on crystal/liquid partitioning of Ru, Rh and Pd for magnetite and hematite solid solutions crystallized from silicate melt. *Chem. Geol.* **113,** 23–43.

Chazey W. J. III. (2004) Platinum-group element geochemistry of large igneous provinces: Source characteristics, geochemical modeling and the role of sulfide saturation. Ph.D. diss. University of Notre Dame.

Chazey W. J. III, Neal C. R., Jain J. C., and Kinman W. S. (2003) A reappraisal of Rb, Y, Zr, Pb and Th values in Geochemical Reference Material BHVO-1. *Geostand. Newsl.* **27,** 181–192.

Chazey W. J. III and Neal C. R. (2004) LIP magma petrogenesis from source to surface: Platinum-group element evidence from Ontong Java Plateau basalts recovered during ODP Leg 192. *J. Geol. Soc. Lond. Spec. Pub.* **229,** 219–238.

Coffin M. F. and Eldholm O. (1993) Scratching the surface: Estimating dimensions of large igneous provinces. *Geology* **21,** 515–518.

Coffin M. F. and Eldholm O. (1994) Large igneous provinces: Crustal structure, dimensions and external consequences. *Rev. Geophys.* **32,** 1–36.

Coffin M. F., Frey F. A., Wallace P. J., Antretter M., Arndt N. T., Barling J., Boehm F., Borre M. K., Coxall H. K., Damuth D., Delius H., Duncan R. A., Inokuchi H., Keszthelyi L., Mahoney J. J., Moore C. L., Müller R. D., Neal C. R., Nicolaysen K. E., Pringle M. S., Reusch D. N., Saccocia P. J., Teagle D. A. H., Wähnert V., Weis D., Wise S. W. Jr., and Zhao X. (2000) *Proceedings of the Ocean Drilling Program: Leg 183 Initial Reports.* Texas A&M University, College Station, TX, USA.

Davies H. L., Sun S-s., Frey F. A., Gautier I., McCulloch M., Price R. C., Bassias Y., Klootwijk C. T., and Leclaire L. (1989) Basalt basement from the Kerguelen Plateau and the trail of the Dupal plume. *Contrib. Mineral. Petrol.* **103,** 457–469.

Devey C. W. Garbe-Schönberg C.-D., Stoffers P., Chauvel C., and Mertz D. F. (1994) Geochemical effects of dynamic melting beneath ridges: Reconciling major and trace element variations in Kolbeinsey (and global) mid-ocean ridge basalt. *J. Geophys. Res.* **99,** 9077–9095.

Duncan R. A. (2002) A time frame for the construction of the Kerguelen Plateau and Broken Ridge. *J. Petrol.* **43,** 1109–1119.

Ely J. C., Neal C. R., O'Neill J. A., and Jain J. C. (1999) Quantifying the platinum group elements (PGEs) and gold in geological samples using cation exchange pretreatment and ultrasonic nebulization inductively coupled plasma-mass spectrometry (USN-ICP-MS). *Chem. Geol.* **157,** 219–234.

Ely J. C. and Neal C. R. (2001) Method of data reduction and uncertainty estimation for platinum-group element (PGE) data using inductively coupled plasma-mass spectrometry (ICP-MS). *Geostand. Newsl.* **26,** 31–39.

Ely J. C. and Neal C. R. (2003) Using platinum group elements to investigate the origin of the Ontong Java Plateau, SW Pacific. *Chem. Geol.* **196,** 235–257.

Ertel W., O'Neill H. St. C., Sylvester P. J., and Dingwell D. B. (1999) Solubilities of Pt and Rh in a haplobasaltic silicate melt at 1300°C. *Geochim. Cosmochim. Acta* **63,** 2439–2449.

Farnetani C. G., Richards M. A., and Ghiorso M. S. (1996) Petrological models of magma evolution and deep crustal structure beneath hotspots and flood basalt provinces. *Earth Planet. Sci. Lett.* **143,** 81–94.

Farnetani C. G., Legras B., and Tackley P. J. (2002) Mixing and deformations in mantle plumes. *Earth Planet. Sci. Lett.* **196,** 1–15.

Fitton J. G. and Godard M. M. (2004) Origin and evolution of magmas on the Ontong Java Plateau. *J. Geol. Soc. Lond. Spec. Pub.* **229,** 151–178.

Frey F. A. and Weis D. (1995) Temporal evolution of the Kerguelen plume: Geochemical evidence from ~38 to 82 Ma lavas forming the Ninetyeast Ridge. *Contrib. Mineral. Petrol.* **121,** 12–28.

Frey F. A. and Weis D. (1996) Reply to the Class et al. discussion of 'Temporal evolution of the Kerguelen Plume: geochemical evidence from ~38 to 82 Ma lavas from the Ninetyeast Ridge'. *Contrib. Mineral. Petrol.* **124,** 104–110.

Frey F. A., McNaughton N. J., Nelson D. R., de Laeter J. R., and Duncan R. A. (1996) Petrogenesis of the Bunbury basalt, Western Australia: Interaction between the Kerguelen plume and Gondwana lithosphere? *Earth Planet. Sci. Lett.* **144,** 163–183.

Frey F. A., Coffin M. F., Wallace P. J., Weis D., Zhao X., Wise S. W. Jr., Wähnert V., Teagle D. A. H., Saccocia P. J., Reusch D. N., Pringle M. S., Nicolaysen K. E., Neal C. R., Müller R. D., Moore

C. L., Mahoney J. J., Keszthelyi L., Inokuchi H., Duncan R. A., Delius H., Damuth J. E., Damasceno D., Coxall H. K., Borre M. K., Boehm F., Barling J., Arndt N. T., and Antretter M. (2000a) Origin and evolution of a submarine large igneous province: The Kerguelen Plateau and Broken Ridge, southern Indian Ocean. *Earth Planet. Sci. Lett.* **176,** 73–89.

Frey F. A., Weis D., Yang H.-J., Nicolaysen K., Leyrit H., and Giret A. (2000b) Temporal geochemical trends in Kerguelen Archipelago basalts: Evidence for decreasing magma supply from the Kerguelen plume. *Chem. Geol.* **164,** 61–80.

Frey F. A., Weis D., Borisova A. Y., and Xu G. (2002) Involvement of continental crust in the formation of the cretaceous Kerguelen Plateau: New perspectives from ODP Leg 120 Sites. *J. Petrol.* **43,** 1207–1239.

Fryer B. J. and Greenough J. D. (1992) Evidence for mantle heterogeneity from platinum-group element abundances in Indian Ocean basalts. *Can. J. Earth Sci.* **29,** 2329–2340.

Gao S., Luo T.-C., Zhang B.-R., Zhang H.-F., Han Y.-W., Zhao Z.-D., and Hu Y.-K. (1998) Chem. composition of the continental crust as revealed by studies in East China. *Geochim. Cosmochim. Acta* **62,** 1959–1975.

Green T. H. (1994) Experimental studies of trace-element partitioning applicable to igneous petrogenesis—Sedona 16 years later. *Chem. Geol.* **117,** 1–36.

Griffiths R. W. and Campbell I. H. (1990) Stirring and structure in mantle starting plumes. *Earth Planet. Sci. Lett.* **99,** 66–78.

Hart S. R. and Ravizza G. E. (1996) Os partitioning between phases in lherzolite and basalt. In *Earth Processes: Reading the Isotopic Code* (eds. A. Basu and S. R. Hart), 123–124. American Geophysical Union, Washington DC, USA.

Hassler D. R. and Shimizu N. (1998) Osmium isotopic evidence for ancient subcontinental lithospheric mantle beneath the Kerguelen islands, Southern Indian Ocean. *Science* **280,** 418–421.

Hill E., Wood B. J., and Blundy J. D. (2000) The effect of Ca-Tschermaks component on trace element partitioning between clinopyroxene and silicate melt. *Lithos* **53,** 203–215.

Hirose K. and Kushiro I. (1993) Partial melting of dry peridotites at high pressures: Determination of compositions of melts segregated from peridotite using aggregates of diamond. *Earth Planet. Sci. Lett.* **114,** 477–489.

Holzheid A. and Grove T. L. (2002) Sulfur saturation limits and their implications for core formation scenarios for terrestrial planets. *Am. Min.* **87,** 227–237.

Ingle S., Weis D., and Frey F. A. (2002) Indian continental crust recovered from Elan Bank, Kerguelen Plateau (ODP Leg 183, Site 1137). *J. Petrol.* **43,** 1241–1257.

Ionov D. A., Hoefs J., Wedepohl K. H., and Wiechert U. (1992) Content and isotopic composition of sulphur in ultramafic xenoliths from central Asia. *Earth Planet. Sci. Lett.* **111,** 289–286.

Jenner G. A., Longerich H. P., Jackson S. E., and Fryer B. J. (1990) ICP-MS—A powerful tool for high-precision trace-element analysis in Earth sciences: Evidence from analysis of selected U. S. G. S. reference samples. *Chem. Geol.* **83,** 133–148.

Keays R. R. (1995) The role of komatiitic and picritic magmatism and S-saturation in the formation of ore deposits. *Lithos* **34,** 1–18.

Keays R. R. and Scott R. B. (1976) Precious metals in ocean ridge basalts: Implications for basalts as source rocks for gold mineralisation. *Econ. Geol.* **71,** 705–720.

Kent R. W., Pringle M. S., Müller R. D., Saunders A. D., and Ghose N. C. (2002) $^{40}Ar/^{39}Ar$ geochronology of the Rajmahal basalts, India and their relationshp to the Kerguelen Plateau. *J. Petrol.* **43,** 1141–1153.

Kumagai I. (2002) On the anatomy of mantle plumes: Effect of the viscosity ratio on entrainment and stirring. *Earth Planet. Sci. Lett.* **198,** 211–224.

Lightfoot P. C., Naldrett A. J., Gorbachev N. S., Doherty W., and Fedorenko V. A. (1990) Geochemistry of the Siberian Trap of the Noril'sk area, USSR, with implications for the relative contributions of crust and mantle to flood basalt magmatism. *Contrib. Min. Petrol.* **104,** 631–644.

Luguet A., Lorand J-P., and Syler M. (2003) Sulfide petrology and highly siderophile element geochemistry of abyssal peridotites: A coupled study of samples from the Kane Fracture Zone (45°W 23°20N, MARK area, Atlantic Ocean). *Geochim. Cosmochim. Acta* **67,** 1553–1570.

Mahoney J. J., Macdougall J. D., Lugmair G. W., and Gopalan K. (1983) Kerguelen hotspot source for Rajmahal Traps and Ninetyeast Ridge? *Nature* **303,** 385–389.

Mahoney J. J., Storey M., Duncan R. A., Spencer K. J., and Pringle M. (1993) Geochemistry and age of the Ontong Java Plateau. In *The Mesozoic Pacific: Geology Tectonics and Volcanism,*pp. 233–261. Geophysical Monograph 77. American Geophysical Union, Washington, DC, USA.

Mahoney J. J., Jones W. B., Frey F. A., Salters V. J. M., Pyle D. G., and Davies H. L. (1995) Geochemical characteristics of lavas from Broken Ridge, the Naturaliste Plateau and southernmost Kerguelen Plateau: Cretaceous plateau volcanism in the southeast Indian Ocean. *Chem. Geol.* **120,** 315–345.

Mattielli N., Weis D., Scoates J. S., Shimizu N., Mennessier J.-P., Grégoire M., Cottin J.-Y., and Giret A. (1999) Evolution of heterogeneous lithospheric mantle in a plume environment beneath the Kerguelen Archipelago. *J. Petrol.* **40,** 1721–1744.

Mavrogenes J. A. and O'Neill H. S. C. (1999) The relative effects of pressure, temperature and oxygen fugacity on the solubility of sulfide in mafic magmas. *Geochim. Cosmochim. Acta* **63,** 1173–1180.

McDonough W. F. and Sun S.-S. (1995) The composition of the Earth. *Chem. Geol.* **120,** 223–253.

Mitchell R. H. and Keays R. R. (1981) Abundance and distribution of gold, palladium and iridium in some spinel and garnet lherzolites: Implications for the nature and origin of precious metal-rich intergranular components in the upper mantle. *Geochim. Cosmochim. Acta* **45,** 2425–2442.

Mohr B. A. R., Wähnert V., Lazarus D. (2002) Mid-Cretaceous paleobotany and palynology of the central Kerguelen Plateau, southern Indian Ocean (ODP Leg 183, Site 1138). *Proc. ODP Sci. Results* **183,** 1–39.

Moore J. G. and Schilling J. G. (1973) Vesicles, water and sulfur in Reykjanes Ridge basalts. *Contrib. Mineral. Petrol.* **41,** 105–118.

Morgan J. W. (1986) Ultramafic xenoliths: Clues to Earth's late accretionary history. *J. Geophys. Res.* **91,** 12375–12387.

Neal C. R. (2001) The interior of the moon: The presence of garnet in the primitive, deep lunar mantle. *J. Geophysical. Res.* **106,** 27865–27885.

Neal C. R., Mahoney J. J., Kroenke L. W., Duncan R. A., and Petterson M. G. (1997) The Ontong Java Plateau. In *Large Igneous Provinces: Continental, Oceanic and Planetary Flood Volcanism,* pp. 183–216. Geophysical Monograph 100. American Geophysical Union, Washington, DC, USA.

Neal C. R., Mahoney J. J., and Chazey W. J. III (2002) Mantle sources and the highly variable role of continental lithosphere in basalt petrogenesis of the Kerguelen Plateau and Broken Ridge LIP: Results from ODP Leg 183. *J. Petrol.* **43,** 1177–1205.

Nicolaysen K., Bowring S., Frey F., Weis D., Ingle S., Pringle M. S., Coffin M. F., and the Leg 183 Scientific Party. (2001) Provenance of Proterozoic garnet-biotite gneiss recovered from Elan Bank, Kerguelen Plateau, southern Indian Ocean. *Geology* **29,** 235–238.

Norman M. D. and Garcia M. O. (1999) Primitive magmas and source characteristics of the Hawaiian plume: Petrology and geochemistry of shield picrites. *Earth Planet. Sci. Lett.* **168,** 27–44.

O'Neill H. St. C. and Mavrogenes J. A. (2002) The sulfide capacity and the sulfur content at sulfide saturation of silicate melts at 1400°C and 1 bar. *J. Petrol.* **43,** 1049–1087.

Peach C. L., Mathez E. A., Keays R. R., and Reeves S. J. (1994) Experimentally determined sulfide melt-silicate melt partition coefficients for iridium and palladium. *Chem. Geol.* **117,** 361–377.

Prichard H. M. and Lord R. A. (1990) Evidence for differential mobility of platinum-group elements in the secondary environment in Shetland ophiolite complex. *Trans. Instn. Min. Metall. Sect. B Appl. Earth Sci.* **103,** B79–B86.

Pringle M. S. and Duncan R. A. (2000) Basement ages from the southern and central Kerguelen plateau and Broken Ridge (abstract). In *2000 Spring Meeting Abstracts.* AGU.

Puchtel I. S., Hofmann A. W., Mezger K., Shchipansky A. A., Kulikov V. S., and Kulikova V. V. (1996) Petrology of a 2.41 Ga remark-

ably fresh komatiitic basalt lava lake in Lion Hills, central Vetreny Belt, Baltic Shield. *Contrib. Mineral Petrol.* **124,** 273–290.

Puchtel I. and Humayun M. (2001) Platinum group element fractionation in a komatiitic basalt lava lake. *Geochim. Cosmochim. Acta* **65,** 2979–2993.

Rehkämper M., Halliday A. N., Barfod D., Fitton J. G., and Dawson J. B. (1997) Platinum-group element abundance patterns in different mantle environments. *Science* **278,** 1595–1598.

Rehkämper M., Halliday A. N., Fitton J. G., Lee D.-C., Wieneke M., and Arndt N. T. (1999) Ir, Ru, Pt and Pd in basalts and komatiites: New constraints for the geochemical behavior of the platinum-group elements in the mantle. *Geochim. Cosmochim. Acta* **63,** 3915–3934.

Rhodes J. M. (1996) Geochemical stratigraphy of lava flows sampled by the Hawaii Scientific Drilling Project. *J. Geophys. Res.***101,** 11729–11746.

Richards M. A., Duncan R. A., and Courtillot V. E. (1989) Flood basalts and hot spot tracks: Plume heads and tails. *Science* **246,** 103–107.

Righter K., Campbell A. J., Humayun M., and Hervig R. L. (2004) Partitioning of Ru, Rh, Pd, Re, Ir, and Au between Cr-bearing spinel, olivine, pyroxene and silicate melts. *Geochim. Cosmochim. Acta* **68,** 867–880.

Roy-Barman M., Wasserburg G. J., Papanastassiou D. A., and Chaussidon M. (1998) Osmium isotopic compostions and Re-Os concentrations in sulfide globules from basaltic glasses. *Earth Planet. Sci. Lett.* **154,** 331–347.

Royer J.-Y., Pierce J. W., Weissel J. K. (1991) Tectonic constraints on hotspot formation of the Ninetyeast Ridge. *Proc. ODP Sci. Results* **121,** 763–776.

Salpeteur I. and Jezequel J. (1992) Platinum and palladium stream-sediment geochemistry downstream from PGE-bearing ultramafics, West Andriamena area, Madagascar. *J. Geochem. Expl.* **43,** 43–65.

Salters V. J. M., Storey M., Sevigny J. H., and Whitechurch H. (1992) Trace element and isotopic characteristics of Kerguelen-Heard Plateau basalts. *Proc. ODP Sci. Results* **120,** 55–62.

Saunders A. D., Storey M., Kent R. W., and Gibson I. L. (1994) Magmatic activity associated with the Kerguelen-Heard plume: Implications for plume dynamics. *Mem. Soc. Geol. France* **166,** 61–72.

Shannon M. C. and Agee C. B. (1998) Percolation of core melts at lower mantle conditions. *Science* **280,** 1059–1061.

Snow J. E. and Schmidt G. (1998) Constraints on Earth accretion deduced from noble metals in the ocean mantle. *Nature* **391,** 166–169.

Storey M., Kent R. W., Saunders A. D., Salters V. J. M., Hergt J., Whitechurch H., Sevigny J. H., Thirlwall M. F., Leat P., Ghose N. C., and Gifford M. (1992) Lower Cretaceous volcanic rocks on continental margins and their relationship to the Kerguelen Plateau. *Proc. ODP Sci. Results* **120,** 33–53.

Subba R. M. V. and Divakara R. V. (1999) Geochemistry and petrogenesis of the basic granulites in the Eastern Ghats mobile belt; extensional environment. In *Eastern Ghats Granulites*(eds. A. T. Rao, V. D. Rao and M. Yoshida), pp. 51–63. Gondwana Research Group Memoir 5. Field Science Publishers, Osaka, Japan.

Sun S-S. and McDonough W.F. (1989) Chemical and isotopic systematics of oceanic basalts: implications for mantle composition and processes. In: Saunders A. D. and Norry M. J. (eds.) *Magmatism in the Ocean Basins. Geol. Soc. London, Special Pub.* **42,** 313–385.

Tatsumi Y., Oguri K., and Shimoda G. (1999) The behaviour of platinum-group elements during magmatic differentiation in Hawaiian tholeiites. *Geochem. J.* **33,** 237–247.

Taufen P. M. and Marchetto C. M. L. (1989) Tropical weathering control of Ni, Cu, Co and platinum group element distributions at the O'Toole Ni-Cu sulphide deposit, Minas Gerais, Brazil. *J. Geochem. Expl.* **32,** 185–197.

Tejada M. L. G., Mahoney J. J., Duncan R. A., and Hawkins M. P. (1996) Age and geochemistry of basement alkalic rocks of Malaita and Santa Isabel, Solomon Islands, Southern Margin of Ontong Java Plateau. *J. Petrol.* **37,** 361–394.

Tejada M. L. G., Mahoney J. J., Neal C. R., Duncan R. A., and Petterson M. G. (2002) Basement geochemistry and geochronology of central Malaita, Solomon Islands, with implications for the origin and evolution of the Ontong Java Plateau. *J. Petrol.* **43,** 449–484.

Tredoux M., Lindsay N. M., Davies G., and McDonald I. (1995) The fractionation of platinum group elements in magmatic systems, with the suggestion of a novel causal mechanism. *S. Afr. J. Geol.* **98,** 157–167.

Tredoux M. and McDonald I. (1996) Komatiite WITS-1, low concentration noble metal standard for the analysis of non-mineralized samples. *Geostand. Newsl.* **20,** 267–276.

Vidale J. E. and Hedlin M. A. H. (1998) Evidence for partial melt at the core-mantle boundary north of Tonga from the strong scattering of seismic waves. *Nature* **391,** 682–685.

Villemant B., Jaffrezic H., Joron J.-L., and Treuil M. (1981) Distribution coefficients of major and trace elements: Fractional crystallization in the alkali basalt series of Chaine des Puys (Massif Central, France). *Geochim. Cosmochim. Acta* **45,** 1997–2016.

Vinnik L., Breger L., and Romanowicz B. (1998) Anisotropic structures at the base of the earth's mantle. *Nature* **393,** 564–567.

Walker R. J., Morgan J. W., and Horan M. F. (1995) Osmium-187 enrichment in some plumes: Evidence for core-mantle interaction? *Science* **269,** 819–821.

Walker R. J., Morgan J. W., Hanski E. J., and Smolkin V. F. (1997) Re-Os systematics of Earyl Proterozoic ferropicrites, Pechenga Complex, northwestern Russia: Evidence for ancient ^{187}Os-enriched plumes. *Geochim. Cosmochim. Acta* **61,** 3145–3160.

Wedepohl K. H. (1995) The composition of the continental crust. *Geochim. Cosmochim. Acta* **59,** 1217–1232.

Weis D., Bassias Y., Gautier I., and Mennessier J.-P. (1989) Dupal anomaly existence 115 MA ago: Evidence from isotopic study of the Kerguelen Plateau (South Indian Ocean). *Geochim. Cosmochim. Acta* **53,** 2125–2131.

Weis D., Frey F. A., Saunders A., Gibson I. L., Dehn J., Driscoll N., Farrell J., Fourtanier E., Gamson P. D., Gee J. S., Janacek T., Klootwijk C., Lawrence J. R., Littke R., Newman J. S., Nomura R., Owen R. M., Peirce J., Popsichal J. J., Rea D. K., Resiwati P., Smit J., Smith G. M., Tamaki K., Taylor E., Weissel J. K., and Wilkinson C. (1991) Ninetyeast Ridge (Indian Ocean); a 5000 km record of a Dupal mantle plume. *Geology* **19,** 99–102.

Weis D., Frey F. A., Leyrit H., and Gautier I. (1993) Kerguelen Archipelago revisited: Geochemical and isotopic study of the Southeast Province lavas. *Earth Planet. Sci. Lett.* **118,** 101–119.

Weis D., Frey F. A., Giret A., and Cantagrel J.-M. (1998) Geochemical characteristics of the youngest volcano (Mount Ross) in the Kerguelen Archipelago: Inferences for magma flux, lithosphere assimilation and composition of the Kerguelen plume. *J. Petrol.* **39,** 973–994.

Weis D., Ingle S., Damasceno D., Frey F. A., Nicolaysen K., and Barling J. (2001) Origin of the continental components in Indian Ocean basalts: Evidence from Elan Bank (Kerguelen Plateau, ODP Leg 183, Site 1137). *Geology* **29,** 147–150.

Weis D. and Frey F. A. (2002) Submarine basalts of the northern Kerguelen Plateau: Interaction between the Kerguelen Plume and the Southeast Indian Ridge revealed at ODP Site 1140. *J. Petrol.* **43,** 1287–1309.

Weis D., Frey F. A., Schlich R., Schaming M., Montigny R., Damasceno D., Mattielli N., and Nicolaysen K. E. (2002) Trace of the Kerguelen mantle plume: Evidence from seamounts between the Kerguelen Archipelago and Heard Island, Indian Ocean. *G^3* **3,** 1–27.

Wood S. A. (1990) The interaction of dissolved platinum with fulvic acid and simple organic acid analogues in aqueous solutions. *Can. Mineral.* **28,** 665–673.

Wood S. A. and Vlassopoulos D. (1990) The dispersion of Pt, Pd and Au in surficial media about two PGE-Cu-Ni prospects in Quebec. *Can. Min.* **28,** 649–663.